

REMARKS

This paper contains corrections of inadvertent errors in Applicants' Fifth Supplementary Amendment submitted March 1, 2004, in response to the Office Action dated February 4, 2000. This is based on a review of Applicants' record copy of this Amendment.

Attachment 21 of the Fifth Supplementary Amendment submitted on March 1, 2004 did not contain all pages it was intended to contain. In attachment A hereto there are the missing pages that should be added to Attachment 21 of the Fifth Supplementary Amendment submitted on March 1, 2004.

Attachment 36 of the Fifth Supplementary Amendment submitted on March 1, 2004 is empty. Attachment B hereto contains what was intended to be contained in Attachment 36 of the Fifth Supplementary Amendment.

In line 8 of page 100 and in the second last line of page 101 of the Fifth Supplementary Amendment submitted on March 1, 2004 after "See Attachment A of Applicants response dated May 14, 1998" there appears "[Attachment 23]." Attachment 23 of the Fifth Supplemental Amendment dated March 4, 2004, does not contain Applicants' response dated May 14, 1998 but only Attachment A thereto.

In line 9 of page 100 and in the last line of page 101 of the Fifth Supplementary Amendment submitted on March 1, 2004 after "See Attachment H of Applicant's response dated November 28, 1997" there appears "[Attachment 24]." Attachment 24 of the Fifth Supplemental Amendment dated March 4, 2004 does not contain Applicants' response dated November 28, 1997 but only Attachment H thereto.

At page 118, four lines from the bottom, after "Poole article [Attachment 21]", it should correctly read "Poole article [Attachment 22]."

At page 172, 9 lines up from the bottom, "Poole Book [Attachment 21]" should correctly read "Poole Book [Attachment 31]."

At page 166, at the end of the last line there should be "[Attachment 44]."

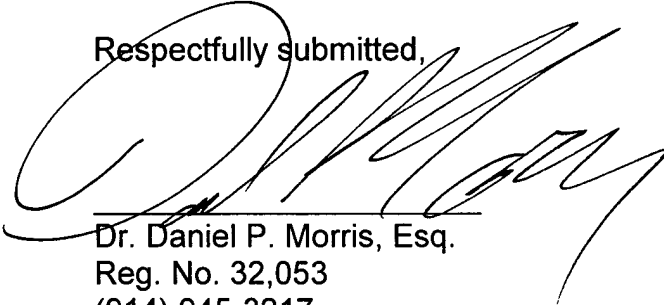
At page 131, last two lines "[Attachment 42]" should correctly read "[Attachment 44]."

At page 173, second line of the last paragraph refers to "Attachment A of their response of December 11, 1998." This is Attachment 29 of the Sixth Supplemental Amendment dated March 1, 2004.

At page 173, fourth line from the last paragraph states "in Attachment 43 of this response there are listed 4 United States Patents with the term "rare earth like" or similar terms in the claims." Attachment 43 does not contain this information. This information is in as Attachment B of the Amendment submitted on November 28, 1997.

Please charge any fee necessary to enter this paper and any previous paper to deposit account 09-0468.

Respectfully submitted,



Dr. Daniel P. Morris, Esq.
Reg. No. 32,053
(914) 945-3217

IBM CORPORATION
Intellectual Property Law Dept.
P.O. Box 218
Yorktown Heights, New York 10598



ATTACHMENT A

COPPER OXIDE SUPERCONDUCTORS

Charles P. Poole, Jr.
Timir Datta
Horacio A. Farach

with help from

M. M. Rigney
C. R. Sanders

Department of Physics and Astronomy
University of South Carolina
Columbia, South Carolina



WILEY

A Wiley-Interscience Publication

JOHN WILEY & SONS

New York • Chichester • Brisbane • Toronto • Singapore

G/

Copyright © 1988 by John Wiley & Sons, Inc.

All rights reserved. Published simultaneously in Canada.

Reproduction or translation of any part of this work beyond that permitted by Section 107 or 108 of the 1976 United States Copyright Act without the permission of the copyright owner is unlawful. Requests for permission or further information should be addressed to the Permissions Department, John Wiley & Sons, Inc.

Library of Congress Cataloging in Publication Data:

Poole, Charles P.

Copper oxide superconductors / Charles P. Poole, Jr., Timir Datta, and Horacio A. Farach; with help from M. M. Rigney and C. R. Sanders.
p. cm.

"A Wiley-Interscience publication."

Bibliography: p.

Includes index.

1. Copper oxide superconductors. I. Datta, Timir. II. Farach, Horacio A. III. Title.

QC611.98.C64P66 1988

539.6'23-dc 19 88-18569 CIP

ISBN 0-471-62342-3

Printed in the United States of America

10 9 8 7 6 5 4 3 2 1

62

7, however,

f the prop-
h they con-
f the other

V

PREPARATION AND CHARACTERIZATION OF SAMPLES

A. INTRODUCTION

Copper oxide superconductors with a purity sufficient to exhibit zero resistivity or to demonstrate levitation (Early) are not difficult to synthesize. We believe that this is at least partially responsible for the explosive worldwide growth in these materials. Nevertheless, it should be emphasized that the preparation of these samples does involve some risks since the procedures are carried out at quite high temperatures, often in oxygen atmospheres. In addition, some of the chemicals are toxic, and in the case of thallium compounds the degree of toxicity is extremely high so ingestion, inhalation, and contact with the skin must be prevented.

The superconducting properties of the copper oxide compounds are quite sensitive to the method of preparation and annealing. Multiphase samples containing fractions with T_c above liquid nitrogen temperature (Monec) can be synthesized using rather crude techniques, but really high-grade single-phase specimens require careful attention to such factors as temperature control, oxygen content of the surrounding gas, annealing cycles, grain sizes, and pelletizing procedures. The ratio of cations in the final sample is important, but even more critical and more difficult to control is the oxygen content. However, in the case of the Bi- and Tl-based compounds, the superconducting properties are less sensitive to the oxygen content.

Figure V-1 illustrates how preparation conditions can influence superconducting properties. It shows how the calcination temperature, the annealing time, and the quenching conditions affect the resistivity drop at T_c of a BiSrCa-CuO pellet, a related copper-enriched specimen, and an aluminum-doped coun-

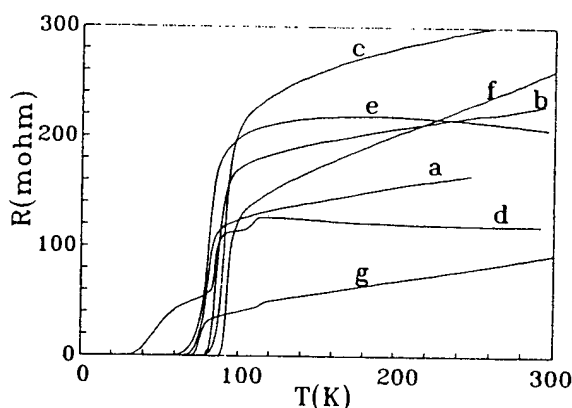


Fig. V-1. Effects of heat treatments on the resistivity transition of $\text{BiSrCaCuO}_{7-\delta}$ (a) calcined at 860°C , (b) calcined at 885°C , (c) calcined at 901°C , (d) aluminum-doped sample calcined at 875°C , prolonged annealing, (e) copper-rich sample calcined at 860°C , (f) aluminum-doped sample calcined at 885°C , slow quenching and (g) calcined at 885°C , prolonged annealing, and slow quenching (Chuz5).

terpart (Chuz5). These samples were all calcined and annealed in the same temperature range and air-quenched to room temperature.

Polycrystalline samples are the easiest to prepare, and much of the early work was carried out with them. Of greater significance is work carried out with thin films and single crystals, and these require more specialized preparation techniques. More and more of the recent work has been done with such samples.

Many authors have provided sample preparation information, and others have detailed heat treatments and oxygen control. Some representative techniques will be discussed.

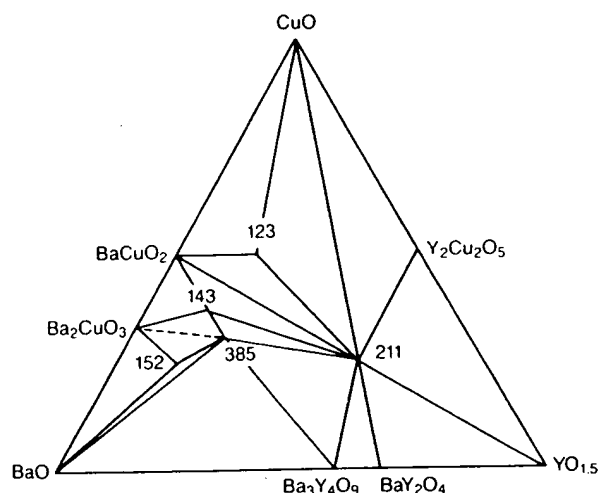
The beginning of this chapter will treat methods of preparing bulk superconducting samples in general, and then samples of special types such as thin films and single crystals. The remainder of the chapter will discuss ways of checking the composition and quality of the samples. The thermodynamic or subsolidus phase diagram of the ternary Y-Ba-Cu oxide system illustrated in Fig. V-2 contains several stable stoichiometric compounds such as the end-point oxides Y_2O_3 , BaO , and CuO at the apices, the binary oxides stable at 950° , $(\text{Ba}_3\text{CuO}_4)$, Ba_2CuO_3 , BaCuO_2 , $\text{Y}_2\text{Cu}_2\text{O}_5$, $\text{Y}_4\text{Ba}_3\text{O}_9$, Y_2BaO_4 , and $(\text{Y}_2\text{Ba}_4\text{O}_7)$, along the edges, and ternary oxides such as $(\text{YBa}_3\text{Cu}_2\text{O}_7)$, the semiconducting green phase Y_2BaCuO_5 , and the superconducting black solid $\text{YBa}_2\text{Cu}_3\text{O}_{7-\delta}$ in the interior (Beye2, Bour3, Capo1, Eagl1, Frase, Hosoy, Jone1, Kaise, Kurth, Kuzzz, Leez3, Lian1, Mali1, Schni, Schn1, Schu1, Takay, Torra, Wagne). Compounds in parentheses are not on the figure, but are reported by other workers. The existence of a narrow range of solid solution was reported (Panso), and then argued against (Wagne) by the same group.

Fig. V-2. Ternary phase $[\text{Y}_2\text{BaCu}]$ other compound:

B. METHODS

In this section the solid-state techniques for preparing superconductors are discussed. The processes in superconductors are discussed at the atomic scale and some families of compounds are more competent.

In the solid-state of the desired compounds, Sr, Tl, Y, or other oxides in nitric



Compound	Slowly cooled to room temperature
123 - $\text{YBa}_2\text{Cu}_3\text{O}_{6.5+\delta}$	O_7
143 - $\text{YBa}_4\text{Cu}_3\text{O}_{8.5+\delta}$	O_9
385 - $\text{Y}_3\text{Ba}_8\text{Cu}_5\text{O}_{17.5+\delta}$	O_{18}
152 - $\text{YBa}_5\text{Cu}_2\text{O}_{8.5+\delta}$	O_9
211 - Y_2BaCuO_5	
$\text{Ba}_2\text{CuO}_{3+\delta}$	$\text{O}_{3.3}$

Fig. V-2. Ternary phase diagram of the Y_2O_3 -BaO-CuO system at 950°C . The green phase [Y_2BaCuO_5 , (211)] the superconducting phase [$\text{YBa}_2\text{Cu}_3\text{O}_{7-\delta}$, (123)], and three other compounds are shown in the interior of the diagram (DeLee).

B. METHODS OF PREPARATION

In this section three methods of preparation will be described, namely, the solid state, the coprecipitation, and the sol-gel techniques (Hatfi). The widely used solid-state technique permits off-the-shelf chemicals to be directly calcined into superconductors, and it requires little familiarity with the subtle physicochemical processes involved in the transformation of a mixture of compounds into a superconductor. The coprecipitation technique mixes the constituents on an atomic scale and forms fine powders, but it requires careful control of the pH and some familiarity with analytical chemistry. The sol-gel procedure requires more competence in analytical procedures.

In the solid-state reaction technique one starts with oxygen-rich compounds of the desired components such as oxides, nitrates, or carbonates of Ba, Bi, La, Sr, Tl, Y, or other elements. Sometimes nitrates are formed first by dissolving oxides in nitric acid and decomposing the solution at 500°C before calcination

(e.g., Davis, Holla, Kelle). These compounds are mixed in the desired atomic ratios and ground to a fine powder to facilitate the calcination process. Then these room-temperature-stable salts are reacted by calcining for an extended period (≈ 20 hr) at elevated temperatures ($\approx 900^\circ\text{C}$). This process may be repeated several times, with pulverizing and mixing of the partially calcined material at each step. As the reaction proceeds, the color of the charge changes. The process usually ends with a final oxygen anneal followed by a slow cool down to room temperature of the powder, or pellets made from the powder, by sintering in a cold or hot press. Sintering is not essential for the chemical process, but for transport and other measurements it is convenient to have the material pelletized. A number of researchers have provided information on this solid-state reaction approach (e.g., Allge, Finez, Galla, Garla, Gopal, Gubse, Hajk1, Hatan, Herrm, Hika1, Hirab, Jayar, Maen1, Mood1, Mood2, Neume, Poepp, Polle, Qadri, Rhyne, Ruzic, Saito, Sait1, Sawa1, Shamo, Takit, Tothz, Wuzz3).

Some of the earlier works on foils, thick films, wires, or coatings employed a suspension of the calcined powder in a suitable organic binder, and the desired product was obtained by conventional industrial processes such as extruding, spraying, or coating.

In the second or coprecipitation process the starting materials for calcination are produced by precipitating them together from solution (e.g., Asela, Bedno, Leez7, Wang2). This has the advantage of mixing the constituents on an atomic scale. In addition the precipitates may form fine powders whose uniformity can be controlled, which can eliminate some of the labor. Once the precipitate has been dried, calcining can begin as in the solid-state reaction procedure. A disadvantage of this method, at least as far as the average physicist or materials scientist is concerned, is that it requires considerable skill in chemical procedures.

Another procedure for obtaining the start-up powder is the sol-gel technique in which an aqueous solution containing the proper ratios of Ba, Cu, and Y nitrates is emulsified in an organic phase and the resulting droplets are gelled by the addition of a high-molecular-weight primary amine which extracts the nitric acid. This process was initially applied to the La materials, but has been perfected for YBaCuO as well (Cimaz, Hatfi).

When using commercial chemical supplies to facilitate the calcination process a dry or wet (acetone) pregrinding with an agate mortar and pestle or a ball mill is recommended. Gravimetric amounts of the powdered precursor materials are thoroughly mixed and placed in a platinum or ceramic crucible. Care must be taken to ensure the compatibility of the ceramic crucible with the chemicals to obviate reaction and corrosion problems.

Complete recipes for the YBa* material have been described (e.g., Gran2). Typically, the mixture of unreacted oxides is calcined in air or oxygen around 900°C for 15 hr. During this time the YBaCuO mixture changes color from the green Y_2BaCuO_5 phase to the dark gray $\text{YBa}_2\text{Cu}_3\text{O}_{7-\delta}$ compound. Then the charge is taken out, crushed, and scanned with X rays to determine its purity. If warranted by the powder pattern X-ray scan, the calcination process is repeated. Often, at this stage the material is very oxygen poor, and electrically it is semi-

conducting or sintered for s at $\approx 3^\circ\text{C}/\text{min}$ temperature is in conductor ph quenching. T sand blasting another oxyg serve the sup

An examf metric amou ing them in a dures several same temper shows the el curve.

WARNING:
precautions i
the high-qua
ides in air at
powdered, a
utes in flowi
perature (Sh
Allen Hei
mation on t
Pharmacol.
antidote fer
cusses cases

C. ADDITI

This section
the prepara

In one e
were calcin
compressio
(Graha). T
 1100°C . Sh
for YBa* a
distinct fro

Another
or Yb, Ba,
tained sub

conducting or even nonconducting. After pelletizing at $>10^5$ psi the pellet is sintered for several hours at $\approx 900^\circ\text{C}$ in flowing oxygen and then slowly cooled at $\approx 3^\circ\text{C}/\text{min}$ down to room temperature. Slow cooling from the elevated temperature is important for producing the low-temperature orthorhombic superconductor phase. The tetragonal nonsuperconducting phase may be obtained by quenching. The pellet may be used as is or it may be cut into suitable sizes by sand blasting, with a diamond saw, or with an arc. After vigorous machining another oxygen anneal (450°C , 1 hr, slow cool down) is often required to preserve the superconducting properties.

An example of preparing a Bi-based superconductor involves mixing gravimetric amounts of high-purity Bi_2O_3 , SrCO_3 , CaCO_3 , and CuO powders, calcining them in air at $750\text{--}890^\circ\text{C}$, regrinding them, and then repeating these procedures several times. Then pellets of the calcined product were sintered at the same temperature and quenched to room temperature (Chuz5). Figure V-1 shows the effect of sample treatment on the resistance versus temperature curve.

WARNING: As was mentioned above, thallium is a toxic material and proper precautions must be taken when working with it. It is useful to start by preparing the high-quality precursor compound BaCu_3O_4 or $\text{Ba}_2\text{Cu}_3\text{O}_5$ by reacting the oxides in air at 925°C for 24 hr. Then appropriate amounts of Tl_2O_3 are added, powdered, and pelletized. The pellet is then heated to $880\text{--}910^\circ\text{C}$ for a few minutes in flowing oxygen, and at the onset of melting it is quenched to room temperature (Shen1).

Allen Hermann has suggested consulting the following references for information on thallium poisoning and antidotes thereto: H. Heydlandf. *Euro. J. Pharmacol.* 6, 340 (1969), which discusses thallium poisoning and describes the antidote ferric cyanoferrate, and *Int. J. Pharmacol.* 10, 1 (1974), which discusses cases of thallium intoxication treated with Prussian Blue.

C. ADDITIONAL COMMENTS ON PREPARATION

This section will treat some additional methods which have been employed for the preparation of samples.

In one experiment coprecipitated nitrates of La, Sr, Cu, and Na carbonate were calcined for 2 hr at 825°C , pressed into pellets, and then subjected to shock compression of ≈ 20 GPa at an estimated peak temperature of $\approx 1000^\circ\text{C}$ (Graham). The best superconductivity was observed after 1 hr of air exposure at 1100°C . Shock compression fabrication has also been reported (Murrz, Murr1) for $\text{YBa}_2\text{Cu}_3\text{O}_{7-x}$ and other rare-earth derivatives. This process produced "monoliths," distinct from the usual composites.

Another technique involved the formation of a precursor alloy of Eu, Ba, Cu or Yb, Ba, Cu by rapid solidification, with the superconducting materials obtained subsequently by oxidation (Halda). A novel method involved preparing

the superconductors from molten Ba-Cu oxides and solid rare-earth-containing materials. In principle this process may be better controlled and complicated shapes can be molded or cast (Herma).

Pulsed current densities of $300\text{--}400 \text{ \AA}/\text{cm}^2$ with rise times of $0.6 \mu\text{sec}$ at room temperature were used to convert the weakly semiconducting phase of YBaCuO to the stable metallic phase (Djure, Djur1).

A claim was made that thermal cycling from cryogenic temperatures to 240 K raised the T_c of YBa* and YBaCuO-F (with some F substituting for O) to 159 K. Cycling above 140 K lowered T_c . This cycling process could possibly change the density of twins and thereby enhance T_c .

A freeze-drying technique was reported as producing sintered materials homogeneous in composition and small in porosity (Stras). The low-temperature firing of oxalates ($T < 780^\circ\text{C}$) has also been reported as producing a homogeneous material of small grain size (Manth).

Both Bi and Pb act as fluxes during the sintering process (Kilco). Bismuth substitution appears to reduce the normal state resistivity by about an order of magnitude without affecting the superconducting properties.

A convenient method of separating the superconducting particles from a powdered mixture using magnetic levitation has been reported (Barso). This may be used to select the superconducting fraction after each calcination process.

D. FILMS

The new ceramic oxide superconductors presently lack mechanical properties such as ductility which are needed for high-current applications like magnet wire fabrication (Jinzz-Jinz3) and power transmission. To circumvent some of these deficiencies for microelectronic applications one can prepare thin films on suitable substrates. Some devices such as Josephson junctions require thin superconducting films. Many workers have discussed the preparation and properties of LaSrCuO- (e.g., Adach, Delim, Kawas, Koinu, Matsu, Nagat, Naito, Tera1) and YBaCuO- (e.g., Burbi, Charz, Evett, Gurvi, Hause, Hongz, Inamz, Kwozz, Kwoz1, Manki, Scheu, Somek, Wuzz4) type films.

Almost every conceivable thin-film deposition technique such as electron beam evaporation, molecular beam epitaxy, sputtering, magnetron, laser ablation, screening, and spraying has been tried with the copper oxide system. Some of these techniques require expensive, elaborate apparatus, although descriptions of simple thin-film deposition systems are also available (e.g., see Koin1). Some representative examples of deposition procedures will be discussed.

Epitaxial films of $\text{YBa}_2\text{Cu}_3\text{O}_{7-\delta}$ on (100) SrTiO_3 were produced using three separate electron beam sources (e.g., Chaud, Chau1, Laibo). The deposition was done in $10^{-4}\text{--}10^{-3}$ torr O_2 with a substrate temperature of 400°C . The deposited films were atomically amorphous with a broad X-ray peak. The epitaxial ordering was achieved upon annealing in O_2 at 900°C with the orthorhombic c axis essentially perpendicular to the plane.

High-quality beam to evaporation (Hammo, O) ited film in oxygen 750°C for 1 hr, furnace.

Superconducting range (Mac) was Ar or an Ar- 10^{-7} torr and, w $\text{ZrO}_2\text{--}9\% \text{ Y}_2\text{O}_3$ films. The films gen annealing. Z erties depended conditions, com

Films of dysprosium beam epitaxy (N) cess was monitored copper was incorporated amorphous Ba a high-temperature

Films of $\text{Y}_{1.1}\text{Ba}_{0.9}\text{Cu}_3\text{O}_{7-\delta}$ with a thickness of 500 \AA were deposited on SrTiO_3 , a pellet of YBaCuO. The evaporation rate was 6 Hz , $\approx 30 \text{ nsec}$ heated to 450°C they appeared slightly oxygen annealed hours. Standard superconductivity tivity achieved 1 LaSr* (Moorj) a

Films were of and Cu in layers 200°C and 10^{-7} layers to diffuse ducting composition conductivity was Y_2O_3 , and BaCu

Some $5000\text{--}10000 \text{ \AA}$ vacuum dc-magnetron was $0.2 \text{ \AA}/\text{sec}$, strate distance

High-quality superconducting films were obtained using a multiple electron beam to evaporate metallic sources in a flow of molecular oxygen at $4-5 \times 10^{-6}$ torr (Hammo, Ohzzz). The deposition rate was 10 \AA/sec . To anneal the deposited film in oxygen it was heated for 3-6 hr in a flow of oxygen at 650°C , raised to 750°C for 1 hr, then to 850°C for 1 hr, and finally slowly cooled down in the furnace.

Superconducting films were prepared using a double ion beam sputtering arrangement (Madak). The target beam was Ar at 40 mA, and the substrate beam was Ar or an Ar- O_2 mixture at 10-500 eV and 2 mA. The base pressure was 5×10^{-7} torr and, with the gas, 4×10^{-4} torr. The best substrate materials such as ZrO_2 -9% Y_2O_3 did not appreciably interact, diffuse, or change the deposited films. The films were $\approx 1 \mu\text{m}$ thick and were rendered superconducting by oxygen annealing. Zero resistance was attained at 88 K. The superconducting properties depended upon the ion beam energy, substrate temperature, annealing conditions, composition, and the extent of poisoning from the substrate.

Films of dysprosium barium copper oxide were grown (Webbz) by molecular beam epitaxy (MBE) using a Varian 360 MBE system, and the nucleation process was monitored by reflection high-energy electron diffraction (RHEED). The copper was incompletely oxidized in metallic microcrystals growing in a sea of amorphous Ba and Dy. After deposition superconducting films were obtained by high-temperature oxygen annealing.

Films of $\text{Y}_{1.1}\text{Ba}_{1.5}\text{Cu}_3\text{O}_{6.4}$ approximately 3300 \AA thick with a surface roughness of 500 \AA were prepared (Dijkk, Inamz, Wuzz4). These films were deposited on SrTiO_3 , sapphire, and vitron carbon by evaporation from a single bulk pellet of YBaCuO 1 cm diameter and 0.2 cm thick at a pressure of 5×10^{-7} torr. The evaporation was produced by several thousand pulses of laser irradiation (3-6 Hz, $\approx 30 \text{ nsec}$ width, 1 J/pulse, 2 J/cm^2). For best results the substrate was heated to 450°C . As deposited thin films were well bonded to the substrate and they appeared shiny dark brown and were electrically insulating. The films were oxygen annealed at 900°C for 1 hr and then slowly cooled over a period of several hours. Standard four-probe resistivity measurements indicated the onset of superconductivity around 95 K and, for a (100) SrTiO_3 substrate, with zero resistivity achieved near 85 K. The laser ablation technique was also employed for LaSr* (Moorj) and YBa* (Nara1).

Films were obtained from sandwiched multilayers by depositing Y_2O_3 , BaO, and Cu in layers (Nasta, Tsaur) on ZrO_2 , MgO, and sapphire substrates at 200°C and 10^{-5} torr. Oxygen treatment for 1-2 hr at $\approx 850^\circ\text{C}$ permitted the layers to diffuse, homogenize, and oxygenate, and thereby form the superconducting compound (Baozz). Films on Ni have also been reported in which superconductivity was obtained by a diffusion process involving the Cu substrate, Y_2O_3 , and BaCO_3 composite (Tachi).

Some 5000- \AA thick films of YBaCuO have been deposited using an ultrahigh vacuum dc-magnetron getter-sputter deposition system. The deposition rate was 0.2 \AA/sec , the substrate temperature was 1050°C , and the target-to-substrate distance was 12 cm. The scattering was done in an Ar- O_2 atmosphere.

The X-ray and electron microscope examinations indicated some variation among the substrates arranged on the heater. Inhomogeneities were observed even within the film made on a single substrate. As deposited the films were oxygen deficient, and annealing produced suitable compositions. The reversible oxygen incorporation was monitored by the systematic splitting of the strongest X-ray peaks. The oxygen diffusion coefficient at 600°C was 10^{-15} m²/sec and the activation energies for desorption and absorption were 1.1 and 1.7 eV, respectively. The highest onset temperature was 99 K with complete superconduction at 40 K. Exposure to water inhibited the superconductor (Barns, Kishi, Yanzz). A device structure with a Y₂O₃ barrier has also been studied (Blami).

Another work showed that films produced by dc magnetron sputtering are copper deficient if the substrate-to-target distance is large or if the substrate is at an elevated temperature (Leez5).

Superconducting YBaCuO thin films with a large surface area (≈ 5 cm \times 5 cm) were grown on Al₂O₃, sapphire, and MgO up to a 500°C substrate temperature by magnetron and diode techniques. Rutherford back scattering (RBS) indicated a uniform composition across magnetron-deposited film areas with diameters up to 5 cm, and the diode film composition homogeneity was even better, but over a smaller area (≈ 2.5 cm diameter). The as-deposited films were annealed in oxygen at different temperatures and exposure times. Prolonged high-temperature annealing ($> 850^\circ\text{C}$) increased the impurity phase. The highest T_c films had a wide range of composition, with the maximum T_c film copper rich. On the basis of an in-situ resistivity study of YBa* thin films a rapid heating to about 900°C in flowing helium followed by slow cool down in flowing oxygen was recommended (David).

The post-deposition anneal cycle was avoided by producing the films in a high-pressure reactive evaporation process involving rapid thermal annealing (Lathr). Smooth films were obtained on zirconia and SrTiO₃ substrates. Screen printing of oxide superconducting films is also possible (Budha, Fuzz1), and simple spray deposition has been reported (Gupta). Films have also been made by coating and spinning off the solutions. Aqueous and aqueous-alcoholic mixed solutions of the metal nitrates (Coop2), metal acetates in dilute acetic acid (Rice1), and sol-gels (Kram1) have all been reported. These processes are potentially important for commercial superconducting coatings on silicon (Kram1), on yttrium-stabilized zirconia (YSZ), on SrTiO₃ (Coop2, Gupta), and on MgO (Gupta, Rice1).

E. SINGLE CRYSTALS

The bulk properties of oxide superconductors are averages over components parallel and perpendicular to the Cu-O planes. In addition, for orthorhombic samples there is an averaging over properties that differ for the a and b directions in this plane. This in-plane anisotropy is especially pronounced for the YBa* 123 structure in which the Cu-O-Cu-O chains lie along the b axis. The

best way to use crystals. Unfortunately anisotropy causes twinning problems in single crystals.

A number of X-ray diffraction (e.g., Crabtree) and micro-Raman spectroscopy studies describe how to grow single crystals. Crystal Growth: Millimeter oxide flux (I Taka4, Zhou) contamination a hot press or (Satoz).

Small single crystals which were sphere and the structure also promotes melting a stage followed by 1

A gold crucible ($1 \times 2 \times 0.1$) was heated in 400°C at 25° on the surface of the crucible.

A detailed crystal by the 1:3 and 2:5 multistep technique found at the crucibles. The crucibles were reported. A single DyBa* as la

F. ALIGNMENT

Clearly high quality of supercon

some variation were observed in the films were . The reversible of the strongest m^2/sec and the 1.7 eV, respectively (Kishi, Yanzz). sputtering are the substrate is at

area ($\approx 5 \text{ cm} \times$ substrate temper- sputtering (RBS) in areas with di- ty was even bet- sited films were mes. Prolonged base. The high- T_c film copper as a rapid heat- in flowing oxy-

g the films in a normal annealing substrates. Screen ia, Fuzz1), and also been made reous-alcoholic dilute acetic acid esses are poten- ilicon (Kram1),), and on MgO

best way to understand these materials is through experiments on perfect single crystals. Unfortunately, untwinned YBa* crystals are not available so the a, b anisotropy cannot be resolved. Tetragonal superconductors should not have this twinning problem. In this work twinned monocrystals will be referred to as single crystals.

A number of experiments have been carried out on monocrystals such as X-ray diffraction (e.g., Borde, Hazen, Lepag, Siegr, Onoda), magnetic studies (e.g., Crabt, Schn1, Worth), mechanical measurements (e.g., Cookz, Dinge), and micro-Raman spectroscopy (e.g., Hemle). In this section we will briefly describe how such crystals are made. The December 1987 issue of the *Journal of Crystal Growth* was devoted to superconductors.

Millimeter-size $(\text{La}_{1-x}\text{Sr}_x)_2\text{CuO}_4$ single crystals were grown in a molten copper oxide flux (Kawa1). Another basic technique employs other fluxes (Haned, Taka4, Zhou1), namely, PbF_2 , B_2O_3 , PbO , PbO_2 , with the risk of possible Pb contamination. LaSr* crystals were also grown by the solid phase reaction using a hot press of pellets (Iwazu) and rapid quenching of a nonstoichiometric melt (Satoz).

Small single crystals of $\text{YBa}_2\text{Cu}_3\text{O}_{7-\delta}$ have been prepared from a sintered powder which was formed into a pellet and then heated, first in a reducing atmosphere and then in an oxidizing one at 925°C . Annealing a stoichiometric mixture also produced monocrystals (Liuzz). Millimeter-size crystals were grown by melting a stoichiometric mixture of $\text{YBa}_2\text{Cu}_3\text{O}_{7-\delta}$ plus excess CuO at 1150°C followed by holding at 900°C for 4 days (Damen, see also Fine1).

A gold crucible on a gold or alumina sheet was used to obtain free-standing ($1 \times 2 \times 0.1 \text{ mm}$) single crystals of YBa* (Kaise, Kais1, Holtz). A charge of 2 g was heated in air at $200^\circ\text{C}/\text{hr}$ and held at 975°C for 1.5 hr, then it was cooled to 400°C at $25^\circ\text{C}/\text{hr}$. The molten charge creeps and forms single crystals and twins on the surfaces. The larger crystals formed in the space between the bottom of the crucible and the gold support sheet.

A detailed account has appeared of the preparation of a 123 compound single crystal by the flux method (Zhou1). The flux mole ratio $\text{BaO}_2:\text{CuO}$ was between 1:3 and 2:5, and the nutrient $\text{Y}_2\text{O}_3:\text{BaO}_2:\text{CuO}$ mole ratios were 0.5:2:3. A multistep temperature process was employed. Black single crystals of YBa* were found at the bottom and at the edge between the wall and the bottom of the crucibles. Platinum crucibles seemed to contaminate the samples so alumina crucibles were recommended. Crystals as large as $2 \times 2 \times 0.3 \text{ mm}^3$ were reported. A similar technique was used to produce single crystals of YBa* and DyBa* as large as 4 mm (Schn1).

F. ALIGNED GRAINS

Clearly high-quality single crystals are important for understanding the physics of superconductors. However, much useful information about anisotropies can

ver components or orthorhombic a and b directions for the b axis. The

be obtained by studying the properties of aligned grains, which are much easier to fabricate.

A superconducting sample can be initially a collection of randomly oriented grains, but various techniques can be used to partially orient these grains so that the c axis lies preferentially in a particular direction. For example uniaxial compression tends to orient compacted grains, with compressed 90- μm particles exhibiting more alignment than compressed 10- μm particles (Glowa). Epoxy-embedded grains have been aligned under the influence of an applied magnetic field and pressure (Arend).

X-ray and magnetic measurements have been reported on aligned crystalline grains of $\text{YBa}_2\text{Cu}_3\text{O}_7$ (Farr1). Optical studies have also been made on aligned grains. The critical current density for samples cut parallel to the compression axis of such grains was nearly isotropic with respect to the direction of an applied magnetic field, and it was a factor of 6 smaller than that for the samples cut perpendicular to this axis (Glowa).

G. REACTIVITY

The oxide superconductors are not inert materials, but rather they are sensitive to exposure to certain gases and to surface contact with particular materials. Great care must be exercised to avoid contamination from water vapor and carbon dioxide in the atmosphere. In addition these materials are catalytic to oxygenation reactions, and these factors result in the occurrence of various chemical and other interactions, especially at elevated temperatures. The granular and porous nature of the materials has an accelerating effect on such reactions.

Samples of YBaCuO may degrade in a matter of days when exposed to an ordinary ambient atmosphere; they react readily with liquid water, acids, and electrolytes, and moderately with basic solutions. The reaction with water (Barns, Kishi, Yanzz) produces nonsuperconducting cuprates. The effects of acetone and other organics (McAnd) have been determined, and stable carboxyl groups have been found in the YBaCuO lattice (Parmi).

Hydrogen enters the YBaCuO lattice at elevated temperatures and forms a solid solution. Low concentrations have very little effect and high concentrations degrade the superconducting properties (Berni, Reill, Yang3). The effects of exposure to oxygen at elevated temperature and oxidation have been discussed several places in this review (e.g., Blend, Engle, Tara3).

The foregoing evidence for the reactivity of the oxide superconductors makes it necessary to consider methods of passivation or protecting them from long-term degradation. An epoxy coating was found to provide some protection (Barns). Coating the surface with metals can be deleterious since metals such as Fe (Gaoz1, Hillz, Weave) and Ti (Meyel) react with the surface of LaSrCuO or YBaCuO . There is evidence for the passivation of the surface of LaSr^* with gold (Meyer).

H. THERM

Thermogravimetric analysis during exposure to oxygen contains an oxidizing atmosphere. The procedures for the method of John4, Leez, differential thermal analysis procedures.

I. CHECKS

After a sample is a conductor. I mine whether the superconducting sample. the magnetic sharp, high $-1/4\pi$. This of the susceptibility the fraction

In addition chemical composition is deduced from material. Cl XPS, electron probe that is investigated; content is much back-scattered, and n

The structure is checked constants a , or orthorhombic indicate a good for LaSr^* (S used to com

H. THERMOGRAVIMETRIC ANALYSIS

Thermogravimetric analysis (TGA) consists of monitoring the weight of a sample during a heating or cooling cycle. For example, one might determine the oxygen content of a superconducting material by measuring its weight change in an oxidizing (O_2 or air) or reducing (e.g., 4% H_2 in Ar) atmosphere. Typical procedures consist of heating or cooling at $20^\circ C/min$. The relative accuracy of the method is about 0.005 (Ongz1). Many workers (e.g., Beye3, Hauck, Huan1, John4, Leez7, Maruc, Ohish, Ongz1, Tara7, Zhuzz) are now using TGA or differential thermal analysis (DTA) routinely during their sample preparation procedures.

I. CHECKS ON QUALITY

After a sample has been prepared it is necessary to check its quality as a superconductor. Most investigators employ the four-probe resistivity check to determine whether it superconducts, and at what temperature it transforms to the superconducting state. A sharp, high T_c transition is an indicator of a high-quality sample. Another widely used quality control method is the determination of the magnetic susceptibility of the specimen. Good quality is indicated by a sharp, high T_c transition with both the flux exclusion and flux expulsion close to $-1/4\pi$. This is, in a sense, a more fundamental check on quality since the value of the susceptibility far below the transition temperature is a good indicator of the fraction of the sample that is superconducting (see Section III-D).

In addition to its superconducting properties, it is also of interest to know the chemical composition and the structure of the specimen. The nominal composition is deduced from the relative proportions of the various cations in the starting material. Chemical analysis and some more sophisticated techniques such as XPS, electro spectroscopic chemical analysis (ESCA), and an electron microprobe that is favorable for low-atomic-weight elements are applicable here. Most investigators only report the cation concentrations in the specimen. Oxygen content is much more difficult to determine, but is important to know. Rutherford back-scattering experiments (John1, Wuzz1, Wuzz4) can provide oxygen contents, and metallography characterizes grain sizes.

The structures of the oxide superconductors described in Chapter VI are easily checked by the X-ray powder pattern method. Many articles list the lattice constants a , b , c of samples and mention whether they are tetragonal ($a = b \neq c$) or orthorhombic ($a \approx b \neq c$). Narrow lines and the absence of spurious signals indicate a good, single-phase sample. Typical X-ray diffraction powder patterns for $LaSr^*$ (Skelt) and YBa^* presented in Figs. V-3 and V-4, respectively, may be used to compare with patterns obtained from freshly prepared samples.

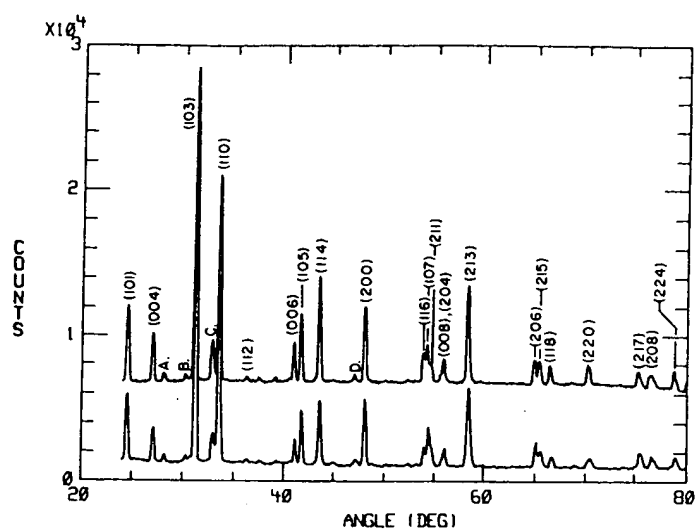


Fig. V-3. Room-temperature (upper curve) and 24-K (lower curve) X-ray diffraction powder patterns of $(\text{La}_{0.925}\text{Ba}_{0.075})_2\text{CuO}_4$ (Skelt).

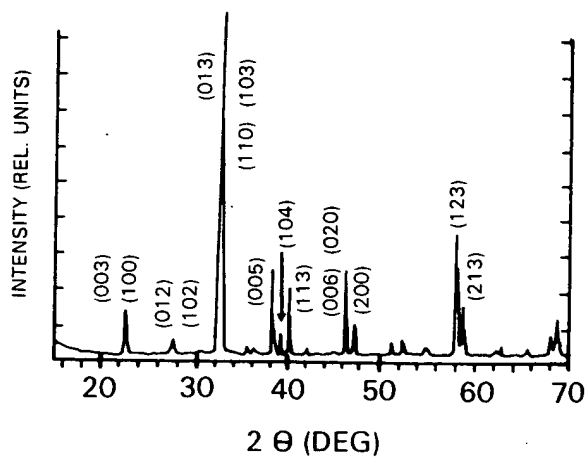


Fig. V-4. Room-temperature X-ray diffraction powder pattern of $\text{YBa}_2\text{Cu}_3\text{O}_7$. (Provided by C. Almasan, J. Estrada, and W. E. Sharp.)

J. RESIST

A measure: temperatur becomes si sharp drop to apply a v such a two Most resist described t method (K silver glazi: portance of port J_c me:

The spe in a suitab: probe conf and out of between tw conducting with the cc ment volta

J. RESISTIVITY MEASUREMENT

A measurement of the resistance $R(T)$ or resistivity $\rho(T)$ of a material versus the temperature is the principal technique employed to determine when a material becomes superconducting. The transition temperature manifests itself by a sharp drop in resistivity to zero. The simplest way to make this measurement is to apply a voltage across the sample and measure the current flow through it, but such a two-probe method (Baszy) is not very satisfactory, and is seldom used. Most resistivity determinations are made with the four-probe technique to be described below, although more sophisticated arrangements such as a six-probe method (Kirsc) can also be used. The fabrication of low-resistance contacts by silver glazing has been reported (Vand2). These researchers pointed out the importance of a low-contact resistance ($\rho < 10 \mu\Omega/\text{mm}^2$ at 77 K) for making transport J_C measurements.

The specimen resistance as a function of temperature is generally determined in a suitable cryostat by attaching leads or electrodes to it in the standard four-probe configuration. Two leads or probes carry a known constant current I into and out of the specimen, and the other two leads measure the potential drop between two equipotential surfaces resulting from the current flow. For superconducting specimens the leads are often arranged in a linear configuration, with the contacts for the input current on the ends, and those for the measurement voltage near the center.

J. J. WATSON RESEARCH CENTER LIBRARY

ray diffraction

U_3O_7 . (Provided

VI

CRYSTALLOGRAPHIC STRUCTURES

A. INTRODUCTION

To properly understand the mechanisms that bring about the superconducting state in particular materials it is necessary to know the structures of the compounds that exhibit this phenomenon. Single-crystal structure studies have been carried out to determine the dimensions of the unit cell, the locations of the atoms in this cell, electronic charge distributions, and the possible presence of atomic irregularities. Neutron powder diffraction has also provided much of the detailed structure information found in this chapter (e.g., Antso, Beech, Cappo, Coxzz, Davi1, Dayzz, Greed, John4, Jorge, Jorg1, Paulz, Torar, Vakni, Yamag, Yanz2). More routine X-ray powder pattern measurements which can identify a known structure and provide the unit cell dimensions are useful for checking the quality of samples, as was explained in Section V-I.

The numerical values of quantities such as lattice parameters and bond lengths show some variation in the literature, and many of our quoted values will be typical ones. Much of the quantitative structural information is organized in the tables.

In the beginning of this chapter we will introduce the perovskite structure and indicate how it is related to the oxide superconductors. Then we will describe the 21 structure of LaSrCuO and the 123 structure of YBaCuO, we will show how each is generated from a perovskite prototype, and we will clarify its layering scheme. The chapter will end with descriptions of the structures of the newer high-transition-temperature bismuth and thallium compounds.

B. PEROVSKITE

Much has been done on the perovskite type structure. This will permit the study of the structures of the

1. Cubic Form

Above 200°C the perovskite is cubic, so the unit cell contains one formula unit in special positions

where we have site which contains atoms, and so 0,0,½ for the oxygen corresponds to the plane center, and as on Fig. VI-1.

named and the constant or length of the space group is

An alternative state texts are

Fig. VI-1. Perovskite edge-centered

B. PEROVSKITES

Much has been written about the oxide superconductor compounds being perovskite types, so we will begin with a description of the perovskite structure. This will permit us to develop some of the notation to be used in describing the structures of the superconductors themselves.

1. Cubic Form

Above 200°C barium titanate crystallizes in the perovskite structure, which is cubic, so the three lattice parameters are all equal (i.e., $a = b = c$). The unit cell contains one formula unit BaTiO_3 and the atoms are located in the following special positions (Wyck2, p. 390):

Ba	(1a)	$\frac{1}{2}, \frac{1}{2}, \frac{1}{2}$	(VI-1)
Ti	(1b)	0,0,0	
O	(3c)	$0, 0, \frac{1}{2}; 0, \frac{1}{2}, 0; \frac{1}{2}, 0, 0$	

where we have employed the crystallographic notation (1a) for an a-type lattice site which contains one atom, (3c) for a c-type lattice site which contains three atoms, and so on. Each atomic position is given by three coordinates, such as $0, 0, \frac{1}{2}$ for the oxygen located at $x = 0, y = 0, z = 0.5a$. This arrangement corresponds to placing a titanium atom on each apex, a barium atom in the body center, and an oxygen atom on the center of each edge of the cube, as illustrated on Fig. VI-1. We see from the figure that the barium atoms are 12-fold coordinated and the titaniums have sixfold (octahedral) coordination. The lattice constant or length of the unit cell is $a = 4.0118 \text{ \AA}$ at 201°C. The crystallographic space group is $Pm\bar{3}m$, O_h^1 .

An alternate way to represent this structure, which is commonly used in solid-state texts and in crystallography monographs (e.g., Wyck2), is to locate the

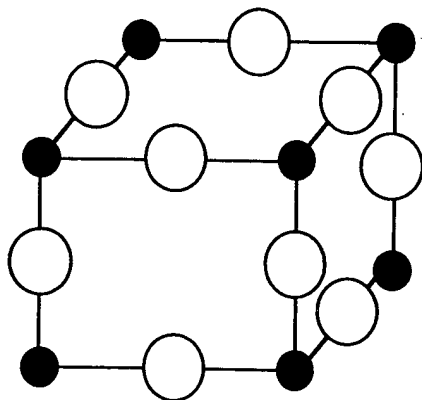


Fig. VI-1. Perovskite cubic unit cell showing titanium on the apices and oxygen in the edge-centered positions. Barium, which is in the body center, is not shown.

origin at the barium site; this places titanium in the center and the oxygens on the centers of the cube faces. The representation (Eq. VI-1) given above is more convenient for comparison with the structures of the oxide superconductors.

The compound $\text{LaBaCu}_2\text{O}_5$ was found to have a cubic perovskite subcell with the lattice parameter $a = 3.917 \text{ \AA}$ (Sishe).

2. Tetragonal Form

At room temperature barium titanate is tetragonal with the unit cell dimensions $a = 3.9947 \text{ \AA}$ and $c = 4.0336 \text{ \AA}$, which is close to cubic. For this lower symmetry the oxygens are assigned to two different sites, a single site along the side edges and a twofold one at the top and bottom. The atomic positions (Wyck2, p. 401)

$$\begin{array}{ll} \text{Ba} & \frac{1}{2}, \frac{1}{2}, 0.488 \\ \text{Ti} & 0, 0, 0 \\ \text{O}(1) & 0, 0, 0.511 \\ \text{O}(2) & 0, \frac{1}{2}, -0.026; \frac{1}{2}, 0, -0.026 \end{array} \quad (\text{VI-2})$$

are shown in Fig. VI-2. The distortions from the ideal structure of Fig. VI-1 are exaggerated on this sketch. We will see later that a similar distortion occurs in the YBaCuO structure. The cubic and tetragonal atom arrangements (VI-1) and (VI-2) are compared in Table VI-1, and we see from this table that the deviation from cubic symmetry is actually quite small.

3. Orthorhombic Form

When barium titanate is cooled below 5°C it undergoes a transition with a further lowering of the symmetry to the orthorhombic space group $\text{Amm}2$, C_{2v} , and

TABLE VI-1. Comparison of Atom Positions of BaTiO_3 in Its Cubic, Tetragonal and Orthorhombic Forms^a

Group	Atom	Cubic and Tetragonal		Cubic	Tetragonal	Orthorhombic
		x	y	z	z	z
TiO_2	Ti	0	0	1	1	1
	O	0	$\frac{1}{2}$	1	0.974	1
	O	$\frac{1}{2}$	0	1	0.974	1
BaO	O	0	0	$\frac{1}{2}$	0.511	$\frac{1}{2}$
	Ba	$\frac{1}{2}$	$\frac{1}{2}$	$\frac{1}{2}$	0.488	$\frac{1}{2}$
TiO_2	Ti	0	0	0	0	0
	O	0	$\frac{1}{2}$	0	-0.026	0
	O	$\frac{1}{2}$	0	0	-0.026	0

^aThe x and y coordinates are the same for both positions. The orthorhombic form z coordinates are also given (Wyck2, pp. 390, 401, 405).

Fig. VI-2. Per

an enlargement
The enlarged c
shown on Fig.
the factor $\sqrt{2}$.
 $5.682 = 4.018$
and the atomic

Ba
Ti
O(1
O(2

where $u = 0$ f

One should
site with differ
of the atoms i
0.490 and 0.5

A compari
cubic to tetra
orthorhombic
tions within x

4. Atom Arra

The ionic rad
together they
smaller Ti^{4+} i
close-packed
empty the latt

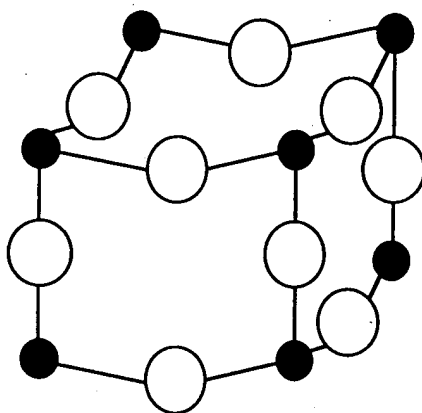


Fig. VI-2. Perovskite tetragonal unit cell showing the puckering of the Ti-O layers.

(VI-2)

Fig. VI-1 are
ion occurs in
ts (VI-1) and
the deviation

an enlargement of the unit cell to accommodate two formula units $(\text{BaTiO}_3)_2$. The enlarged cell is rotated by 45° relative to the higher-temperature ones, as shown on Fig. VI-3, and therefore its a and b lattice parameters are larger by the factor $\sqrt{2}$. The three lattice constants are $a = 5.669 = 4.009\sqrt{2} \text{ \AA}$, $b = 5.682 = 4.018\sqrt{2} \text{ \AA}$, and $c = 3.990 \text{ \AA}$. There are no longer any special sites, and the atomic positions are (Wyck2, p. 405):

$$\begin{array}{llll}
 \text{Ba} & (2a) & 0, \frac{1}{2}, \frac{1}{2}; \frac{1}{2}, 0, \frac{1}{2} & \\
 \text{Ti} & (2b) & 0, u + \frac{1}{2}, 0; \frac{1}{2}, u, 0 & \text{with } u = 0.510 \\
 \text{O(1)} & (2a) & 0, u + \frac{1}{2}, \frac{1}{2}; \frac{1}{2}, u, \frac{1}{2} & \text{with } u = 0.490 \\
 \text{O(2)} & (4e) & u, v + \frac{1}{2}, 0; -u, v + \frac{1}{2}, 0; u + \frac{1}{2}, v, 0; -u + \frac{1}{2}, v, 0 & \\
 & & \text{with } u = 0.253, v = 0.237 &
 \end{array} \quad (\text{VI-3})$$

on with a fur-
m2, C_{2v} , and

where $u = 0$ for Ba.

One should note that in Eq. (VI-3) Ba and O(1) are in the same (2a) type of site with different values of the parameter u . Figure VI-3 shows the coordinates of the atoms in the orthorhombic cell drawn using the approximation $\approx \frac{1}{2}$ for 0.490 and 0.510 and $\approx \frac{1}{4}$ for 0.253 and 0.237.

A comparison of Eqs. VI-1 to VI-3 indicates that the transformation from cubic to tetragonal involves only shifts in the z coordinates of atoms, while the orthorhombic phrase differs from the cubic one only through shifts in atom positions within x, y planes (see Table VI-1).

4. Atom Arrangements

The ionic radii of Ba^{2+} (1.34 \AA) and O^{2-} (1.32 \AA) are almost the same, and together they form a face-centered cubic (fcc) close-packed lattice with the smaller Ti^{4+} ions (0.68 \AA) located in octahedral holes. The octahedral holes of a close-packed oxygen lattice have a radius of 0.545 \AA , and if these holes were empty the lattice parameter would be $a = 3.73$, as shown on Fig. VI-4a. If each

tragonal and

horhombic

z

1

1

1

$\frac{1}{2}$

$\frac{1}{2}$

0

0

0

z coordinates are

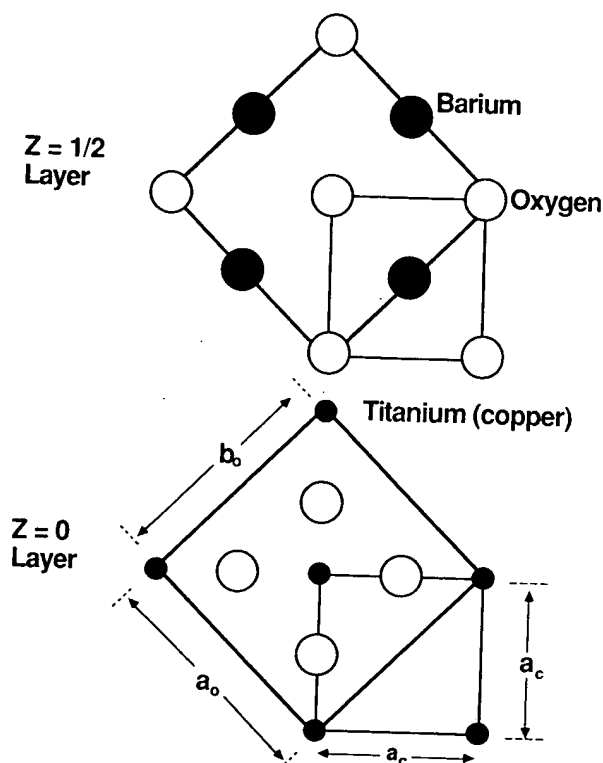


Fig. VI-3. Atom positions of perovskite when the monomolecular tetragonal unit cell is expanded to the bimolecular orthorhombic cell with new axes at 45° with respect to the old ones.

titanium were to move the surrounding oxygens apart to its ionic radius when occupying the hole, as shown on Fig. VI-4b, the lattice parameter a would be 4.00 \AA . The observed cubic ($a = 4.012 \text{ \AA}$) and tetragonal ($a = 3.995 \text{ \AA}$, $c = 4.034 \text{ \AA}$) lattice parameters are close to these values, indicating a pushing apart of the oxygens. The tetragonal distortion illustrated on Fig. VI-2 and the orthorhombic distortion of Eq. (VI-3) constitute attempts to achieve this through an enlarged but distorted octahedral site. This same mechanism is operative in the oxide superconductors.

C. BARIUM-LEAD-BISMUTH OXIDE

In 1983 Mattheiss and Hamann referred to the 1975 "discovery by Sleight et al. of high temperature superconductivity" of the compound $\text{BaPb}_{1-x}\text{Bi}_x\text{O}_3$ in the composition range $0.05 \leq x \leq 0.3$ with T_c up to 13 K (Matt7, Sleig). Many consider this system, which disproportionates $2 \text{ Bi}^{4+} \rightarrow \text{Bi}^{3+} + \text{Bi}^{5+}$ in going from the metallic to the semiconducting state, as a predecessor to the LaSrCuO system.

Fig. VI-4. The dral hole and (the hole. For e parameter is g

Crystal s
 BaPbO_3 has
 and at room
 $6.136 = 4.35$
 $\beta = 90.17^\circ$ (
 and has wha
 4.35 \AA). Th
 at room temp
 tetragonal to

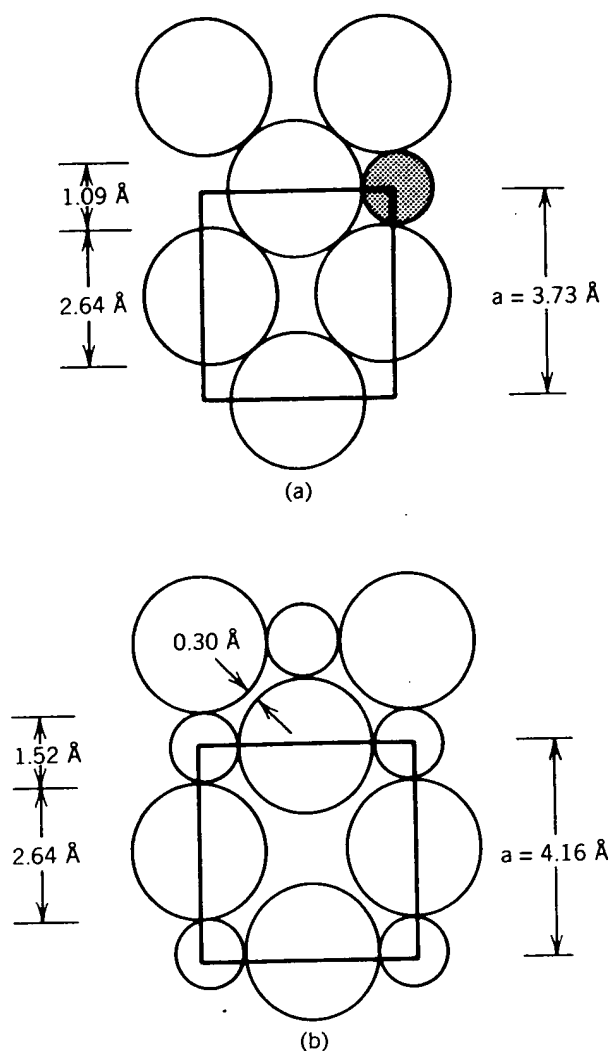


Fig. VI-4. The $z = 0$ plane of the perovskite unit cell showing (a) the size of the octahedral hole and (b) the pushing apart of the oxygens by the presence of a transition ion in the hole. For each case the oxygen and hole sizes are indicated on the left and the lattice parameter is given on the right.

Crystal structure determinations indicate that the metallic compound BaPbO_3 has the cubic perovskite structure with $a = 4.273 \text{ \AA}$ (Wyck2, p. 391), and at room temperature semiconducting BaBiO_3 is monoclinic with $a = 6.136 = 4.339\sqrt{2} \text{ \AA}$, $b = 6.181 = 4.371\sqrt{2} \text{ \AA}$, $c = 8.670 = 4.335 \times 2 \text{ \AA}$, and $\beta = 90.17^\circ$ (Coxz1, Coxz2). The latter is quite close to orthorhombic ($\beta = 90^\circ$), and has what might be called a pseudocubic perovskite lattice parameter ($a = 4.35 \text{ \AA}$). These two compounds form a solid solution series $\text{BaPb}_{1-x}\text{Bi}_x\text{O}_3$ which at room temperature changes as a function of increasing x from orthorhombic to tetragonal to orthorhombic to monoclinic. Superconductivity appears in the

tetragonal phase, and the metal-to-insulator transition occurs at the tetragonal-to-orthorhombic phase boundary $x \approx 0.35$ (Matt7, Sleil).

D. PEROVSKITE-TYPE SUPERCONDUCTING STRUCTURES

In their first report on high-temperature superconductors Bednorz and Müller referred to their samples as "metallic, oxygen deficient . . . perovskite like mixed valent copper compounds." Subsequent work has confirmed that the new superconductors do indeed have these characteristics. In this section we will comment on their perovskite-like aspects.

1. Atom Sizes

In the oxide superconductors Cu replaces the Ti^{4+} ions (0.68 \AA) of perovskite, and in most cases retains the CuO_2 layering with two oxygens per copper in the layer. Other cationic replacements tend to be Bi, Ca, La, Sr, Tl, and Y for the larger Ba, forming "layers" containing only one oxygen or none per cation. We see from the following list of ionic radii

Cu^{2+}	0.72 \AA	
Bi^{5+}	0.74 \AA	
Y^{3+}	0.94 \AA	
Tl^{3+}	0.95 \AA	
Bi^{3+}	0.96 \AA	
Ca^{2+}	0.99 \AA	(VI-4)
Sr^{2+}	1.12 \AA	
La^{3+}	1.14 \AA	
Ba^{2+}	1.34 \AA	
O^{2-}	1.32 \AA	

that there are four size groups, with all other cations significantly smaller than the Ba of perovskite. The common feature of CuO_2 layers that are planar or close to planar establishes a fairly uniform lattice size in the a, b plane. The parameters of the compounds $LaSrCuO$ ($a = b = 3.77 \text{ \AA}$), $YBaCuO$ ($a = 3.83 \text{ \AA}$, $b = 3.89 \text{ \AA}$), $BiSrCaCuO$ ($a = b = 3.82 \text{ \AA}$), and $TlBaCaCuO$ ($a = b = 3.86 \text{ \AA}$) are all between the ideal fcc oxygen lattice value of 3.73 \AA and the perovskite one of 4.01 \AA .

Table VI-2 gives the ionic radii of the positively charged ions of various elements of the periodic table. These radii are useful for estimating changes in lattice constant when ionic substitutions are made in existing structures. They also provide some insight into which types of substitutions will be most favorable.

TABLE VI-2.
Charge States^a

Z	Eler
3	I
11	M
19	I
37	I
55	C
4	
12	
20	
38	
56	
5	
13	
31	
49	
81	
6	
14	
32	
50	
82	
15	
33	
51	
83	
16	
34	
52	
21	
22	
23	
24	
25	

TABLE VI-2. Ionic Radii in Angstroms of Selected Elements for Various Positive Charge States^a

Z	Element	+1	+2	+3	+4	+5	+6
<i>Alkali</i>							
3	Li	0.68					
11	Na	0.97					
19	K	1.33					
37	Rb	1.47					
55	Cs	1.67					
<i>Alkaline earths</i>							
4	Be	0.44	0.35				
12	Mg	0.82	0.66				
20	Ca	1.18	0.99				
38	Sr		1.12				
56	Ba	1.53	1.34				
<i>Group III</i>							
5	B	0.35		0.23			
13	Al			0.51			
31	Ga	0.81		0.62			
49	In			0.81			
81	Tl	1.47		0.95			
<i>Group IV</i>							
6	C				0.16		
14	Si	0.65			0.42		
32	Ge		0.73		0.53		
50	Sn		0.93		0.71		
82	Pb		1.20		0.84		
<i>Group V</i>							
15	P			0.44		0.35	
33	As			0.58		0.46	
51	Sb	0.89		0.76		0.62	
83	Bi	0.98		0.96		0.74	
<i>Chalcogenides</i>							
16	S				0.37		0.30
34	Se	0.66			0.50		0.42
52	Te	0.82			0.70		0.56
<i>First transition series (3dⁿ)</i>							
21	Sc			0.81			
22	Ti	0.96	0.94	0.76	0.68		
23	V		0.88	0.74	0.63	0.59	
24	Cr	0.81	0.89	0.63			0.52
25	Mn		0.80	0.66	0.60		

TABLE VI-2. (continued)

Z	Element	+1	+2	+3	+4	+5	+6
26	Fe		0.74	0.64			
27	Co		0.72	0.63			
28	Ni		0.69				
29	Cu	0.96	0.72				
30	Zn	0.88	0.74				
<i>Second transition series (4dⁿ)</i>							
39	Y			0.94			
40	Zr	1.09			0.79		
41	Nb	1.00			0.74	0.69	
42	Mo	0.93			0.70		0.62
43	Tc						
44	Ru				0.67		
45	Rh			0.68			
46	Pd		0.80		0.65		
47	Ag	1.26	0.89				
48	Cd	1.14	0.97				
<i>Third transition series (5dⁿ)</i>							
72	Hf				0.78		
73	Ta					0.68	
74	W						
75	Re				0.70		0.62
76	Os				0.72		
77	Ir				0.88		0.69
78	Pt		0.80		0.68		
79	Au	1.37		0.85	0.65		
80	Hg	1.27	1.10				
<i>Rare earths (4fⁿ)</i>							
57	La	1.39		1.14			
58	Ce	1.27		1.07	0.94		
59	Pr			1.06	0.92		
60	Nd			1.04			
61	Pm			1.06			
62	Sm			1.00			
63	Eu			0.98			
64	Gd			0.62			
65	Tb			0.93	0.81		
66	Dy			0.92			
67	Ho			0.91			
68	Er			0.89			
69	Tm			0.87			
70	Yb			0.86			
71	Lu			0.85			

*Three anion radii are 1.32 for O²⁻, 1.33 for F⁻, and 1.84 for S²⁻ (*Handbook of Chemistry and Physics*).

2. Unit Cell

Three and four conducting units removed in the cell to be less

YB:

LaS

Similar structure

E. LANTHANUM

The structure is usually described by the structure of the corresponding superconducting divalent cation. The structure is usually described by the structure of the corresponding superconducting divalent cation. The structure is usually described by the structure of the corresponding superconducting divalent cation.

The compound is usually described by the structure of the corresponding superconducting divalent cation. The structure is usually described by the structure of the corresponding superconducting divalent cation. The structure is usually described by the structure of the corresponding superconducting divalent cation.

1. Tetragonal

The tetragonal structure of K₂NiF₄ is described by the structure of the corresponding superconducting divalent cation. The structure is usually described by the structure of the corresponding superconducting divalent cation. The structure is usually described by the structure of the corresponding superconducting divalent cation.

with $u = 0.1$, $c = 13.18$ Å. The structure is usually described by the structure of the corresponding superconducting divalent cation. The structure is usually described by the structure of the corresponding superconducting divalent cation. The structure is usually described by the structure of the corresponding superconducting divalent cation.

2. Unit Cell Stacking

Three and four fundamental fcc unit cells stack vertically to form the superconducting unit cells of YBaCuO and LaSrCuO, respectively, with some oxygens removed in the process. This causes the vertical height or c parameter of the unit cell to be less than that expected for the stacking of perovskite cells:

$$\begin{array}{lcl} \text{YBaCuO:} & c \approx 11.7 \text{ \AA}, 3c_{\text{fcc}} = 11.19 \text{ \AA}, 3c_{\text{per}} = 12.03 \text{ \AA} \\ \text{LaSrCuO:} & c \approx 13.18 \text{ \AA}, 4c_{\text{fcc}} = 14.92 \text{ \AA}, 4c_{\text{per}} = 16.04 \text{ \AA} \end{array} \quad (\text{VI-5})$$

Similar stackings occur in the BiSrCaCuO and TlBaCaCuO compounds.

E. LANTHANUM-COPPER OXIDE

The structure of LaSrCuO, $(\text{La}_{1-x}\text{M}_x)_2\text{CuO}_{4-\delta}$, called the 21 structure, where M is usually Sr or Ba, is tetragonal in some cases and orthorhombic in others. We will describe the tetragonal case first and then the orthorhombic distortion of it. The structures will be described in terms of the prototype compound La_2CuO_4 corresponding to $x = \delta = 0$ in the above expression, keeping in mind that in the superconducting compounds themselves some of the La atoms are replaced by a divalent cation such as Sr or Ba. Since lanthanum has a charge of +3 and oxygen is -2, it follows that all of the copper is divalent (+2) when $x = 0$, and some becomes trivalent for $x > 0$.

The compound La_2CuO_4 itself is considered to be nonsuperconducting, but some investigators claim that it or portions of it do exhibit superconductivity, perhaps of a filamentary type (Beill, Coop1, Dvora, Gran1, Pick1, Shahe, Skelt, Skell1, Skell2).

1. Tetragonal Form

The tetragonal LaSrCuO superconductors crystallize in what is called the K_2NiF_4 structure with space group $I4/mmm$, D_{4h}^{17} and two formula units per unit cell (e.g., Burns, Coll1, Hirot, Mossz, Onoda; Wyck3, p. 68). The copper atoms and one of the oxygen types O(1) are in special positions and the remaining atoms are all in general positions, with a single undetermined parameter associated with the z coordinate. The positions are

$$\begin{array}{lll} \text{La} & (4e) & 0,0,u; 0,0,-u; \frac{1}{2},\frac{1}{2},u+\frac{1}{2}; \frac{1}{2},\frac{1}{2},-u+\frac{1}{2} \\ \text{Cu} & (2a) & 0,0,0; \frac{1}{2},\frac{1}{2},\frac{1}{2} \\ \text{O(1)} & (4c) & 0,\frac{1}{2},0; \frac{1}{2},0,0; \frac{1}{2},0,\frac{1}{2}; 0,\frac{1}{2},\frac{1}{2} \\ \text{O(2)} & (4e) & 0,0,v; 0,0,-v; \frac{1}{2},\frac{1}{2},v+\frac{1}{2}; \frac{1}{2},\frac{1}{2},-v+\frac{1}{2} \end{array} \quad (\text{VI-6})$$

with $u = 0.362$ and $v = 0.182$. Typical lattice dimensions are $a = b = 3.77 \text{ \AA}$, $c = 13.18 \text{ \AA}$. Table VI-3 gives more details on the atom positions and Fig. VI-5a provides a sketch of this 21 structure. Table VI-4 lists the measured lattice

TABLE VI-3. Atom Positions of Regular and Alternate La_2CuO_4 Structure, Both of Which Correspond to Space Group $I4/mmm$, D_{4h}^{17a}

Complex	Ideal z	Regular Structure					Alternate Structure				
		Atom	Site	x	y	z	Atom	Site	x	y	z
CuO_2	1	O(1)	4c	$\frac{1}{2}$	0	1	O(1)	4c	$\frac{1}{2}$	0	1
		O(1)	4c	0	$\frac{1}{2}$	1	O(1)	4c	0	$\frac{1}{2}$	1
OLa	$\frac{5}{6} = 0.833$	Cu	2a	0	0	1	Cu	2a	0	0	1
		La	4e	$\frac{1}{2}$	$\frac{1}{2}$	0.862	La	4e	$\frac{1}{2}$	$\frac{1}{2}$	0.862
LaO	$\frac{2}{3} = 0.667$	O(2)	4e	$\frac{1}{2}$	$\frac{1}{2}$	0.682	O(2)	4d	0	$\frac{1}{2}$	$\frac{3}{4}$
		La	4e	0	0	0.638	O(2)	4d	$\frac{1}{2}$	0	$\frac{3}{4}$
O_2Cu	$\frac{1}{2}$	O(1)	4c	0	$\frac{1}{2}$	$\frac{1}{2}$	La	4e	0	0	0.638
		O(1)	4c	$\frac{1}{2}$	0	$\frac{1}{2}$	O(1)	4c	0	$\frac{1}{2}$	$\frac{1}{2}$
LaO	$\frac{1}{3} = 0.333$	Cu	2a	$\frac{1}{2}$	$\frac{1}{2}$	$\frac{1}{2}$	O(1)	4c	$\frac{1}{2}$	0	$\frac{1}{2}$
		La	4e	0	0	0.362	Cu	2a	$\frac{1}{2}$	$\frac{1}{2}$	$\frac{1}{2}$
OLa	$\frac{1}{6} = 0.167$	O(2)	4e	$\frac{1}{2}$	$\frac{1}{2}$	0.318	La	4e	0	0	0.362
		La	4e	0	0	0.182	O(2)	4d	$\frac{1}{2}$	0	$\frac{1}{4}$
CuO_2	0	O(1)	4c	$\frac{1}{2}$	0	0	O(2)	4d	0	$\frac{1}{2}$	$\frac{1}{4}$
		O(1)	4c	0	$\frac{1}{2}$	0	La	4e	$\frac{1}{2}$	$\frac{1}{2}$	0.138
		Cu	2a	0	0	0	O(1)	4c	$\frac{1}{2}$	0	0
							O(1)	4c	0	$\frac{1}{2}$	0
							Cu	2a	0	0	0

^aSuperconducting compounds crystallize in the regular structure (Oguch; see also Onoda). The ideal z values in column 2 are for the prototype perovskite.

constants for tetragonal LaSrCuO superconductors with various values of x , y , and δ in the formula $(\text{La}_{1-x}\text{Sr}_x)_{2-y}\text{CuO}_{4-\delta}$.

2. Alternate Tetragonal Form

In the previous section we discussed the tetragonal structure which is adopted by LaSrCuO superconductors. It has a variant (Hutir, Oguch) called the Nd_2CuO_4 structure in which the oxygens O(2) are in special sites (4d) instead of the general (4e) sites in the same space group, corresponding to

$$\text{O}(2) \quad (4d) \quad 0, \frac{1}{2}, \frac{1}{4}; \frac{1}{2}, 0, \frac{1}{4}; \frac{1}{2}, 0, \frac{3}{4}; 0, \frac{1}{2}, \frac{3}{4} \quad (\text{VI-7})$$

The remaining atoms are in the positions given by Eq. (VI-6) and listed in Table VI-3, and the unit cell is sketched on the right-hand side of Fig. VI-5. This structure tends to be unstable relative to its K_2NiF_4 counterpart, and is not known to superconduct.

Fig. VI-5.
with the su
the right (C
the two cel

3. Orthor

The 21 ort
logue give
structure
means tha
ones, and
similar to
5.409 Å :
times $\sqrt{2}$:
bic values
little char
orthorhon

listed in c

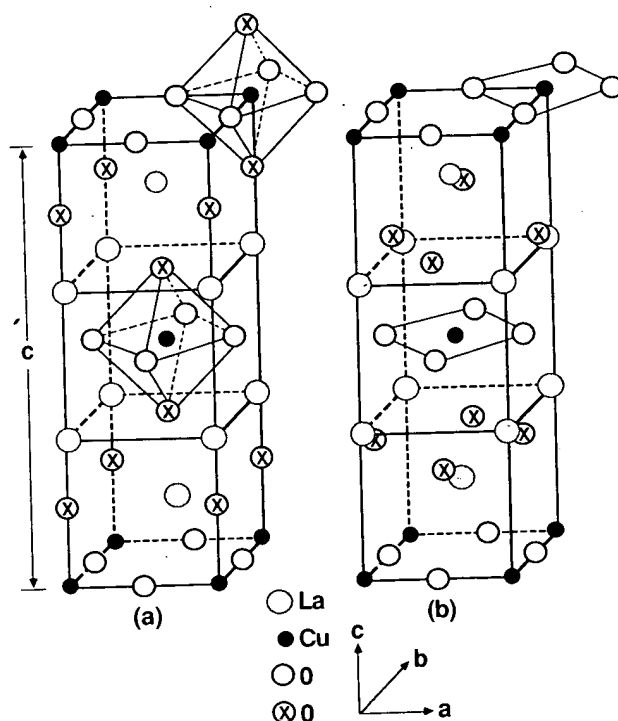


Fig. VI-5. Lanthanum copper oxide tetragonal unit cell. The regular cell (a) associated with the superconducting compounds is shown on the left and the alternative one (b) is on the right (Oguchi; see also Ohba1). The oxygens denoted by \otimes have different positions in the two cells.

3. Orthorhombic Form

The 21 orthorhombic LaSrCuO structure (Longo) is related to its tetragonal analogue given by Eq. (VI-6) in the same way that the orthorhombic perovskite structure (VI-3) is related to its tetragonal (VI-2) and cubic (VI-1) forms. This means that the orthorhombic basis directions are at 45° relative to the tetragonal ones, and the number of formula units in the cell is doubled. The situation is similar to that described by Fig. VI-3, with $a = 5.363 \text{ \AA} = 3.792\sqrt{2} \text{ \AA}$, $b = 5.409 \text{ \AA} = 3.825\sqrt{2} \text{ \AA}$, $c = 13.17 \text{ \AA}$. Writing the a and b lattice parameters times $\sqrt{2}$ compensates for the new choice of axes and shows that the orthorhombic values are close to the tetragonal $a = 3.81 \text{ \AA}$ given earlier. There is also very little change in c . Table VI-5 lists the measured lattice constants for several orthorhombic compounds. The anisotropy factors ANIS

$$\text{ANIS} = \frac{100 |b - a|}{0.5 (b + a)} \quad (\text{VI-8})$$

listed in column 6 give the percentage deviation from tetragonality.

T. J. WATSON RESEARCH CENTER LIBRARY

TABLE VI-4. Selected Lattice Parameters for $(R_{1-x}M_x)_2CuO_{4-\delta}$ Type Superconductors with Tetragonal Structure^a

R-M	x	Lattice Parameters ^b		Ref.
		$a = b$ (Å)	c (Å)	
Y-Ba	0.4	3.828	12.68	Allge
La-Ba	0.05	3.782	13.168	Skelt
	0.075	3.7817	13.2487	Yuzzz
	0.075	3.787	13.31	Fujit
	0.1	3.791	13.35	Fujit
La-Sr	0.05	3.7839	13.211	Tara1
	0.05	3.78	13.25	Hidak
	0.063	3.7784	13.216	Tara1
	0.075	3.7793	13.2	Decro
	0.075	3.7771	13.226	Tara1
	0.075	3.776	13.234	Shelt
	0.075	3.772	13.247	Brunz
	0.087	3.7739	13.232	Tara1
	0.1	3.7739	13.23	Tara1
	0.1	3.777	13.2309	Przys
	0.112	3.7708	13.242	Tara1
	0.125	3.7685	13.247	Tara1
	0.132	3.7666	13.255	Tara1
	0.15	3.7657	13.259	Tara1

^aThe table is sorted by cations and then by increasing x , the dopant parameter (prepared by M. M. Rigney).

^bThe a and b lattice parameters were converted from measured values of a_0 , b_0 of Fig. VI-3 through the expression $a = a_0/\sqrt{2}$, $b = b_0/\sqrt{2}$.

Copper atoms and one of the oxygen types O(1) are in special positions; the remaining two atoms La and O(2) are in general positions with a single undetermined parameter associated with the z coordinate. The space group is $Fmmm$, D_{2h}^{23} , and the positions of the atoms are as follows:

$$\begin{array}{ll}
 \text{La} & (8i) \quad 0,0,u; 0,\frac{1}{2},\frac{1}{2}+u; \frac{1}{2},0,\frac{1}{2}+u; \frac{1}{2},\frac{1}{2},u; \\
 & \quad 0,0,-u; 0,\frac{1}{2},\frac{1}{2}-u; \frac{1}{2},0,\frac{1}{2}-u; \frac{1}{2},\frac{1}{2},-u \\
 \text{Cu} & (4a) \quad 0,0,0; 0,\frac{1}{2},\frac{1}{2}; \frac{1}{2},0,\frac{1}{2}; \frac{1}{2},\frac{1}{2},0 \\
 \text{O(1)} & (8e) \quad \frac{1}{4},\frac{1}{4},0; \frac{1}{4},\frac{3}{4},\frac{1}{2}; \frac{3}{4},\frac{1}{4},\frac{1}{2}; \frac{3}{4},\frac{3}{4},0 \\
 & \quad \frac{1}{4},\frac{1}{4},\frac{1}{2}; \frac{1}{4},\frac{3}{4},0; \frac{3}{4},\frac{1}{4},0; \frac{3}{4},\frac{3}{4},\frac{1}{2} \\
 \text{O(2)} & (8i) \quad 0,0,v; \dots \text{ (same as La with } v \text{ replacing } u)
 \end{array} \quad (VI-9)$$

where the parameters $u = 0.362$ and $v = 0.182$ have the same values as in the tetragonal case presented above. Since u and v are the same and the lattice constants are so close to the tetragonal values, the sketch of the tetragonal unit cell in Fig. VI-5a applies here also. Another work (Hirotsu, see also Onoda) assigned

TABLE VI-5. Selected Lattice Parameters for $(La_{0.9}Ba_{0.1})_2CuO_4$ with the Orthorhombic Structure^a

R-M	x
La-Ba	0.0
	0.0
	0.0
La-Ba	0.1
La-Ca	0.0

^aANIS is the anisotropy.

^bThe a and b lattice parameters were converted from measured values of a_0 , b_0 of Fig. VI-3 through the expression $a = a_0/\sqrt{2}$, $b = b_0/\sqrt{2}$.

$$(La_{0.9}Ba_{0.1})_2CuO_4 \\
 5.408 = 3.824$$

4. Phase Transition

The compound $(La_{0.9}Ba_{0.1})_2CuO_4$ has been studied by Dayzz, Dvora, and others. The phase transition temperature has been determined to be 3.824 K.

Fig. VI-6. Phase transition line for $(La_{0.9}Ba_{0.1})_2CuO_4$. The spin-density wave transition temperature has been determined to be 3.824 K.

TABLE VI-5. Selected Lattice Parameters for $(R_{1-x}M_x)_2CuO_{4-\delta}$ Type Superconductors with the Orthorhombic Structure^a

Ref.	R-M	x	Lattice Parameters			ANIS	Ref.
			a (Å)	b (Å)	c (Å)		
Allge	La-Ba	0.02	3.786	3.811	13.17	0.66	Fujit
Skelt		0.075	3.786*	3.808*	13.257	0.58	Shelt
Yuzzz		0.075	3.798*	3.803*	13.234	0.13	Onoda
Fujit	La-Ba	0.1	3.786*	3.824*	13.264	1.00	Hiroto
Fujit	La-Ca	0.075	3.772*	3.808*	13.168	0.95	Shelt

^aANIS is the anisotropy factor $100|b - a|/0.5(b + a)$ (prepared by M. M. Rigney).

^bThe a and b lattice parameters were converted from the measured values of a_0 , b_0 of Fig. VI-3 through the expressions $a = a_0/\sqrt{2}$, $b = b_0/\sqrt{2}$.

$(La_{0.9}Ba_{0.1})_2O_4$ to the space group $Pccm$, D_{2h}^{31} with $a = 5.354 = 3.786\sqrt{2}$ Å, $b = 5.408 = 3.824\sqrt{2}$ Å, and $c = 13.264$ Å.

4. Phase Transition

The compounds $(La_{1-x}M_x)_2CuO_4$ with $M = Sr$ and Ba are orthorhombic at low temperatures and low M contents, and tetragonal otherwise, and superconductivity has been found on both sides of this transition (Baris, Bedn3, Birge, Dayzz, Dvora, Fujit, Gree1, Kangz, Koyam, Mihal, Paulz; see also Heldz). The prototype compound La_2CuO_4 itself also exhibits the tetragonal-to-orthorhombic transition. The phase diagram of Fig. VI-6 shows the tetragonal, orthorhombic

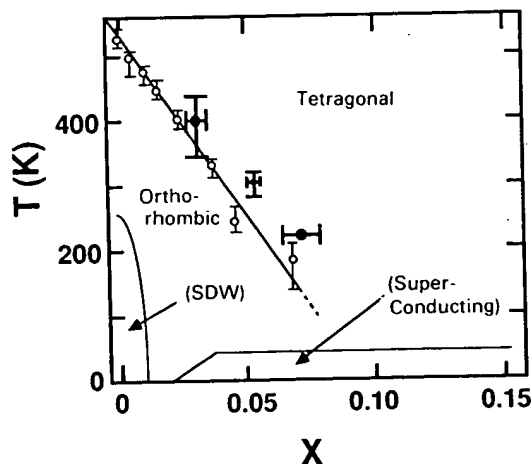


Fig. VI-6. Phase diagram showing data points along the tetragonal-to-orthorhombic transition line for $(La_{1-x}Ba_x)_2CuO_{4-\delta}$ (○, Fujit) and $(La_{1-x}Sr_x)_2CuO_4$ (●, Moret). The spin-density wave (SDW) and superconducting ● regions are indicated. These two compounds have about the same superconducting region.

bic, superconducting, and spin-density wave (SDW) regions for the barium compound (Fujit), and data points for the strontium compound (Moret, More8). An alternate phase diagram has been proposed (Ahar1). Alkaline metal contents much larger than those shown on the figure (e.g., $x \approx 0.5$) can be non-superconducting. The SDW region occurs below the minimum concentration for the onset of superconductivity. Another work (Geise) showed that LaSr(0.04) undergoes a structural phase transition between 180 and 300 K.

5. Generation of LaSrCuO Structures

The LaSrCuO tetragonal structures may be visualized as being derived from four LaCuO₃ perovskite unit cells of the type illustrated in Fig. VI-1 stacked one above the other along the z or c axis. To generate La₂CuO₄ in the K₂NiF₄ structure the layers of CuO₂ atoms on the $z = \frac{1}{4}$ and $z = \frac{3}{4}$ levels of this four-cell stacking are removed, La and O are interchanged on two other layers, and the middle layer Cu atom is shifted from the edge to the center point $(\frac{1}{2}, \frac{1}{2}, \frac{1}{2})$ of the unit cell. Then the cell is compressed vertically from 14.9 to 13.2 Å (Table VI-4) to take up the space formerly occupied by the removed CuO₂ layers. Finally, the lanthanums along the c axis and the oxygens along the side edges are shifted vertically to accommodate the new atom arrangement.

To generate La₂CuO₄ with the Nd₂CuO₄ arrangement from this same four-cell stacking all of the oxygens on the vertical edges are removed, and two lanthanums are moved to edge sites. Copper is handled the same way as before, so in both cases the generated structure lacks two CuO₂ layers.

6. Layering Scheme of LaSrCuO

When we described the LaSrCuO structures we left out what is perhaps their most important characteristic, namely, their layered aspect. Lanthanum copper oxide may be looked upon as consisting of Cu-O layers of square-planar coordinated copper ions with lanthanum and O(2)-type oxygen ions populating the spaces between the layers. These Cu-O layers are stacked equally spaced, perpendicular to the c axis, as shown in Fig. VI-7, and their oxygens are aligned along the c axis, as indicated by the vertical dotted line on the left side of the figure. The copper ions, on the other hand, are not aligned vertically, but rather alternate between (000) and $(\frac{1}{2}, \frac{1}{2}, \frac{1}{2})$ sites in adjacent layers, as illustrated in Figs. VI-5 and VI-7.

The copper is actually octahedrally coordinated with oxygen, but the Cu-O distance of 1.9 Å in the CuO₂ planes is much less than the vertical distance of 2.4 Å between copper and the oxygens above and below, as shown in Fig. VI-8. When the structure is distorted orthorhombically the Cu-O spacings in both the planes and the c direction remain quite close to their tetragonal counterparts.

The copper ions and the O(1)-type oxygens in the planes are both in special sites in the tetragonal and orthorhombic forms, in accordance with Eqs. (VI-6) and (VI-9), and as a result the plane is perfectly flat in both cases. When the

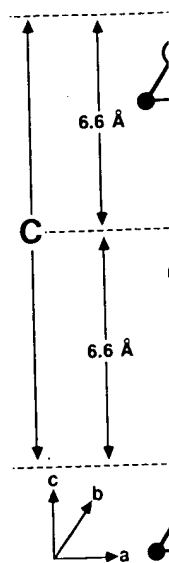


Fig. VI-7. La perpendicular

structure is course the pl planes could

The copp indicated on octahedra. The su planes are themselves.

F. YTTRIU

The YBaCu terparts, cc scribed in t perovskite defect struc

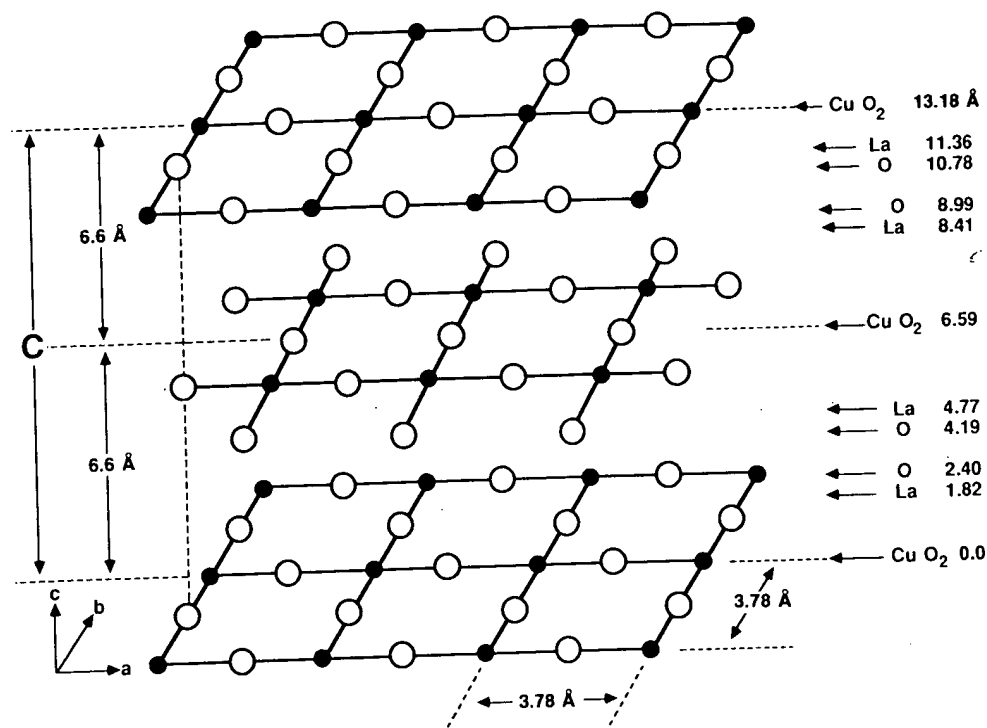


Fig. VI-7. Layering scheme of the LaSrCuO superconducting structure. The layers are perpendicular to the c axis.

structure is tetragonal the square-planar arrangement is also perfect, and of course the planes are perfectly parallel to each other. These characteristics of the planes could influence the superconducting properties.

The copper-oxygen planes are bound together by Cu-O and La-O bonds, as indicated on Fig. VI-5, and Fig. VI-8 shows the spacial arrangement of the CuO₆ octahedra. This figure also makes clear how the copper ions alternate along the c axis. The superconducting properties are probably less influenced by the way the planes are bound together than by the internal characteristics of the planes themselves.

F. YTTRIUM-BARIUM-COPPER OXIDE

The YBaCuO compounds such as Y_{1-x}Ba_{2-y}Cu₃O_{7-δ}, like their LaSrCuO counterparts, come in tetragonal and orthorhombic varieties, and both will be described in turn. Then we will show how to generate the structures from their perovskite prototypes, we will explain the layering scheme, and finally related defect structures will be discussed.

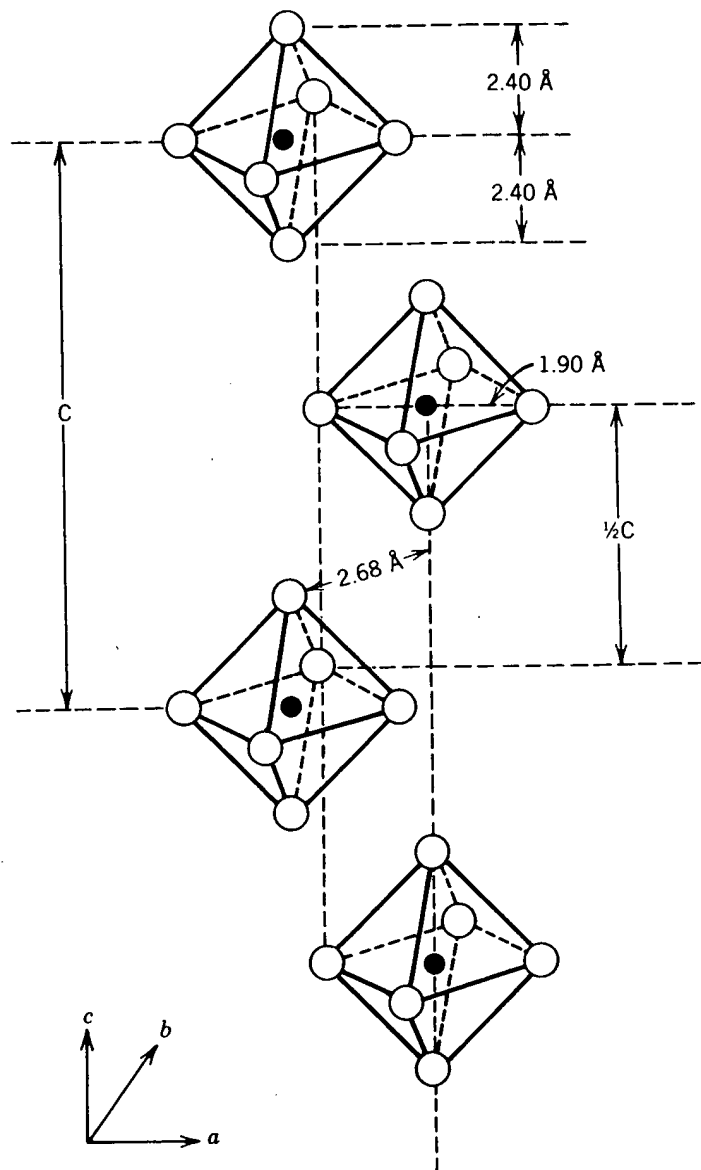


Fig. VI-8. Ordering of the LaSrCuO copper atoms and their associated octahedra of oxygen nearest neighbors along the c axis. The LaSrCuO structure consists of alternately displaced octahedra with axes parallel to c .

In much of the early work the formula $\text{YBa}_2\text{Cu}_3\text{O}_{9-\delta}$ was used for YBaCuO because there are nine oxygens in the prototype perovskite structure. When the crystallographers showed that the 14-atom unit cell of YBaCuO contains 8 oxygen sites, the formula $\text{Y}_1\text{Ba}_2\text{Cu}_3\text{O}_{8-\delta}$ began being widely used, and finally when structure refinements demonstrated that one of the oxygen sites is systematically vacant, the more appropriate expression $\text{Y}_1\text{Ba}_2\text{Cu}_3\text{O}_{7-\delta}$ was introduced, and it is the one that we will use throughout this work.

The orthorhombic structure is reported to occur at 81 K (Xiao3 phase transition) replacing the tetragonal structure (Fein1, Ovshi).

1. Tetragonal

The tetragonal structure with $\delta > 0.5$ was first reported by earlier assignments, and the parameter

The u, v, w, z coordinates of the unit cell are reported by only partly of this structure. The lack of yttrium atoms in VI-2.

The semi-empirical D_{4h}^1 (Borde, version of one that none really "ideal" perovskite fit to

The correct formula $\text{Cu}_6\text{O}_{14-\delta}$ (Ivantsyural with the

The orthorhombic phase is ordinarily superconducting. There are, however, some reported exceptions: (1) doping with gallium in copper chain sites can induce the orthorhombic-to-tetragonal transformation with T_c remaining as high as 81 K (Xiao3); (2) replacing one oxygen by sulfur in $\text{EuBa}_2\text{Cu}_3\text{O}_{7-\delta}$ induces this phase transformation with a small change in T_c from 92 to 85 K (Fel'n2); and (3) replacing one oxygen with two fluorines to form $\text{YBa}_2\text{Cu}_3\text{O}_6\text{F}_2$ could produce a tetragonal structure with all eight oxygen sites occupied and an enhanced T_c (Fel'n1, Ovshi).

1. Tetragonal Form

The tetragonal $\text{YBa}_2\text{Cu}_3\text{O}_{7-\delta}$ structure, which is stable above about 650°C with $\delta > 0.5$, was assigned to space group $P4/mmm$, D_{4h}^1 (Jorge, see Eagle, Lepad). Earlier assignments were $P4m2$, D_{2d}^5 or possibly $P4mm$, C_{4v}^1 (Hazen). There is one formula unit per unit cell. Yttrium and one copper atom are in special positions, and the remaining atoms are all in general positions with a single undetermined parameter associated with the z coordinate of each:

Y	(1d)	$\frac{1}{2}, \frac{1}{2}, \frac{1}{2}$		
Ba	(2h)	$\frac{1}{2}, \frac{1}{2}, u; \frac{1}{2}, \frac{1}{2}, -u$	$u = 0.1914$	
Cu(t)	(1a)	0,0,0		
Cu(m)	(2g)	0,0, v ; 0,0, $-v$	$v = 0.3590$	(VI-10)
O(t)	(2f)	$0, \frac{1}{2}, 0; \frac{1}{2}, 0, 0$		
O(m,m')	(4i)	$0, \frac{1}{2}, w; \frac{1}{2}, 0, w$ $0, \frac{1}{2}, -w; \frac{1}{2}, 0, -w$	$w = 0.3792$	
O(b)	(2g)	0,0, x ; 0,0, $-x$	$x = 0.1508$	

The u , v , w , and x parameters (from Jorge) are used in column 10 of Table VI-6. The unit cell dimensions are $a = 3.9018 \text{ \AA}$, $c = 11.9403 \text{ \AA}$ (Jorge), and those reported by other investigators are listed in Table VI-7. Oxygen site O(t) may be only partly occupied. The atom positions are given in Table VI-6 and a sketch of this structure is presented on the right side of Fig. VI-9. The oxygen sites in the basal plane at $z = 0$ are about half occupied in a random or disordered manner. The lack of planarity of the CuO_2 layers immediately below and above the yttrium atom is reminiscent of tetragonal perovskite, which is sketched in Fig. VI-2.

The semiconducting compound $\text{YBa}_2\text{Cu}_3\text{O}_6$ was also assigned to $P4/mmm$, D_{4h}^1 (Borde, Renau, Swinn, Torar), as shown in the table. This is a tetragonal version of orthorhombic $\text{YBa}_2\text{Cu}_3\text{O}_7$ formed by removing the chain oxygens so that none remain on the basal plane. A claim has been made (Relle) that the "ideal" perovskite z values shown in column 6 of Table VI-6 provide an adequate fit to X-ray powder diffraction data from $\text{YBa}_2\text{Cu}_3\text{O}_7$.

The compounds $\text{La}_3\text{Ba}_3\text{Cu}_6\text{O}_{14+\delta}$ (David, see also Golb1), $(\text{La}_{0.4}\text{Ba}_{0.6})_6\text{Cu}_6\text{O}_{14-\delta}$ (Iwaz3), and $\text{LaBa}_2\text{Cu}_{3-x}\text{O}_{7-\delta}$ (Nakai) have been reported as isostructural with tetragonal $\text{YBa}_2\text{Cu}_3\text{O}_8$.

octahedra of
alternately

for YBaCuO
re. When the
contains 8 oxy-
l finally when
systematically
iced, and it is

TABLE VI-6. Atom Positions of $\text{YBa}_2\text{Cu}_3\text{O}_{7-\delta}$ in its Orthorhombic (Superconducting) and Tetragonal Forms^a

Layer	Atom	Site	x	y	Ideal z	z	Average ^b	Jorge	Jorge	Hazen	Borde ^c
CuO_2	$\text{O}(t)$	1e	$\frac{1}{2}$	0	1	1 + w	1	1	1	1.03	—
	$\text{Cu}(t)$	1a	0	0	1	1	1	1	1	1.00	1
	$\text{O}(t')$	1b	0	$\frac{1}{2}$	1	1 - w	1	1	1	0.97	—
BaO	$\text{O}(b)$	2q	0	0	$\frac{1}{2} = 0.8333$	1 - z	0.8432	0.8458	0.8492	0.85	0.8460
	Ba	2t	$\frac{1}{2}$	$\frac{1}{2}$	$\frac{1}{2} = 0.8333$	1 - u	0.8146	0.8105	0.8086	0.81	0.8079
	$\text{Cu}(m)$	2q	0	0	$\frac{1}{2} = 0.6667$	1 - v	0.6445	0.6426	0.6410	0.64	0.6395
CuO_2	$\text{O}(m')$	2r	0	$\frac{1}{2}$	$\frac{1}{2} = 0.6667$	1 - x	0.6219	0.6196	0.6208	0.62	0.6206
	$\text{O}(m)$	2s	$\frac{1}{2}$	0	$\frac{1}{2} = 0.6667$	1 - y	0.6210	0.6233	0.6208	0.61	0.6206
	$\text{O}(y)$	—	0	0	$\frac{1}{2}$	—	—	—	—	—	—
Y	Y	1h	$\frac{1}{2}$	$\frac{1}{2}$	$\frac{1}{2}$	$\frac{1}{2}$	$\frac{1}{2}$	$\frac{1}{2}$	$\frac{1}{2}$	$\frac{1}{2}$	$\frac{1}{2}$
	$\text{O}(m)$	2s	$\frac{1}{2}$	0	$\frac{1}{2} = 0.333$	y	0.3790	0.3767	0.3792	0.39	0.3794
	$\text{O}(m')$	2r	0	$\frac{1}{2}$	$\frac{1}{2} = 0.333$	x	0.3781	0.3804	0.3792	0.38	0.3794
CuO_2	$\text{Cu}(m)$	2q	0	0	$\frac{1}{2} = 0.333$	v	0.3555	0.3574	0.3590	0.36	0.3605
	Ba	2t	$\frac{1}{2}$	$\frac{1}{2}$	$\frac{1}{2} = 0.1667$	u	0.1854	0.1895	0.1914	0.19	0.1921
	$\text{O}(b)$	2q	0	0	$\frac{1}{2} = 0.1667$	z	0.1568	0.1542	0.1508	0.15	0.1540
CuO_2	$\text{O}(t)$	1b	$\frac{1}{2}$	0	0	w	0	0	0	0.03	—
	$\text{Cu}(t)$	1a	0	0	0	0	0	0	0	0	0
	$\text{O}(t')$	1e	0	$\frac{1}{2}$	0	-w	0	0	0	-0.03	—
δ					-2	-1	0	$0 < \delta < 0.5$	$0.5 < \delta < 1$	+0.5	+1.0
a (Å)							3.827	3.8591	3.9018	3.859	3.8715
b (Å)							3.882	3.9195	3.9018	3.859	3.8715
c (Å)							11.682	11.8431	11.9403	11.71	11.738

^aColumn 8 gives the average z values of several investigators for $\delta = 0$. Values are also given for $\delta = 0.5$, and 1.0. The ideal z is for the prototype perovskite $\text{YBa}_2\text{Cu}_3\text{O}_6$ shown on the left side of Fig. VI-11.

^bThe average assumes z of $\text{O}(m)$ is greater than z of $\text{O}(m')$. Various authors differ on this point (e.g., Jorge).

^c $\text{Y}_{0.9}\text{Ba}_{2.1}\text{Cu}_3\text{O}_6$.

TABLE VI-7. Tetragonal Str

R-M

Y-Ba

Dy-Ba

Er-Ba

Eu-Ba

Gd-Ba

Ho-Ba

Tm-Ba

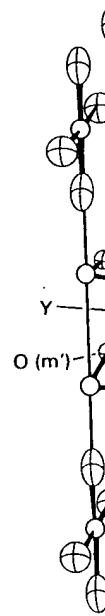
^aThe table is sorted^bThe a and b lattice expressions

Fig. VI-9. S copper oxide basal plane: the atoms.

TABLE VI-7. Selected Lattice Parameters for $\text{RBa}_2\text{Cu}_3\text{O}_{7-\delta}$ Type Copper Oxides with Tetragonal Structure^a

R-M	δ	$a = b$ (Å)	c (Å)	Ref.
Y-Ba	0.5	3.859	11.71	Hazen
	0.5	3.859	11.71	Hemle
	—	3.87 ^b	11.67	Ihar2
	0.0	3.87 ^b	11.67	Hirab
Dy-Ba	0.72	3.8656	11.783	Tara3
Er-Ba	0.84	3.854	11.796	Tara3
Eu-Ba	0.41	3.86	11.73	Boole
Gd-Ba	0.48	3.877	11.81	Tara3
Ho-Ba	0.87	3.8601	11.791	Tara3
Tm-Ba	0.93	3.8491	11.788	Tara3

^aThe table is sorted by cations (prepared by M. M. Rigney).

^bThe a and b lattice parameters were converted from the measured values a_0 , b_0 of Fig. VI-3 through the expressions $a = a_0/\sqrt{2}$, $b = b_0/\sqrt{2}$.

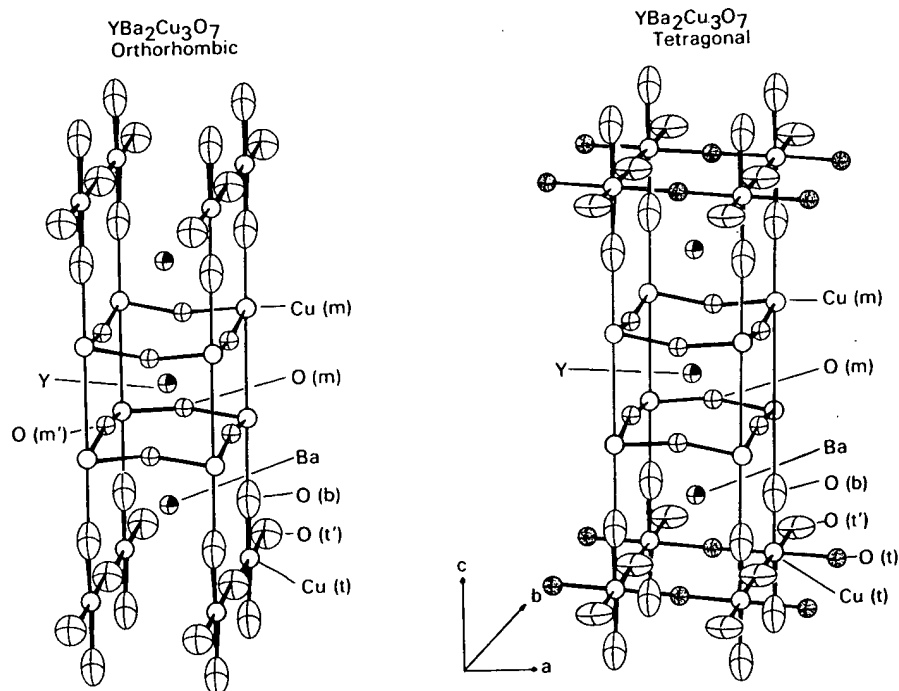


Fig. VI-9. Sketches of the orthorhombic (left) and tetragonal (right) yttrium-barium-copper oxide unit cells. (Adapted from Jorg1.) Oxygens are randomly dispersed over the basal plane sites in the tetragonal structure. Thermal vibration ellipsoids are shown for the atoms.

Column 8 gives the average z values of several investigators for $\delta = 0$. Values are also given for $\delta = 0.5$, and 1.0. The ideal z is for the prototype perovskite $\text{YBa}_2\text{Cu}_3\text{O}_6$ shown on the left side of Fig. VI-11.
^bThe average assumes z of $\text{O}(m)$ is greater than z of $\text{O}(m')$. Various authors differ on this point (e.g., Jorgé).
^c $\text{Y}_{0.9}\text{Ba}_{2.1}\text{Cu}_3\text{O}_6$.

2. Orthorhombic Form

Orthorhombic $\text{YBa}_2\text{Cu}_3\text{O}_8$ with the 123 structure was assigned to the space group $Pmmm$, D_{2h}^1 (Antso, Beech, Benoz, Cales, Cappo, Coxzz, Greed, Jorge, Siegr, Yosh3, Yanz2, Youzz) with one formula unit per unit cell and the representative lattice parameters $a = 3.827 \text{ \AA}$, $b = 3.882 \text{ \AA}$, and $c = 11.682 \text{ \AA}$. Yttrium, one copper, and two oxygens are in special positions, and the remaining atoms are all in general positions with a single undetermined parameter associated with the z coordinate:

$$\begin{array}{llll}
 \text{Y} & (1h) & \frac{1}{2}, \frac{1}{2}, \frac{1}{2} & \\
 \text{Ba} & (2t) & \frac{1}{2}, \frac{1}{2}, u; \frac{1}{2}, \frac{1}{2}, -u & u = 0.1854 \\
 \text{Cu}(t) & (1a) & 0, 0, 0 & \\
 \text{Cu}(m) & (2q) & 0, 0, v; 0, 0, -v & v = 0.3555 \\
 \text{O}(t) & (1b) & \frac{1}{2}, 0, 0 & \\
 \text{O}(t') & (1e) & 0, \frac{1}{2}, 0 & \\
 \text{O}(m') & (2r) & 0, \frac{1}{2}, x; 0, \frac{1}{2}, -x & x = 0.3790 \\
 \text{O}(m) & (2s) & \frac{1}{2}, 0, y; \frac{1}{2}, 0, -y & y = 0.3781 \\
 \text{O}(b) & (2q) & 0, 0, z; 0, 0, -z & z = 0.1568
 \end{array} \quad (\text{VI-11})$$

The u , v , x , y , and z parameters correspond to the average atom positions given in column 8 of Table VI-6. Lattice dimensions a , b , and c and atom positions for several structure determinations are given in Table VI-6. Table VI-8 lists lattice parameters for a number of orthorhombic YBaCuO compounds. Variable temperature crystallographic data are also available (Antso, Cappo, Hewa1, Jorge, Jorg1, Momin, Renau). Sketches of this structure are presented on the left side of Fig. VI-9 (see also Steil). We see from this figure that the $\text{O}(t)$ oxygen site is empty, which corresponds to the presence of $-\text{Cu}-\text{O}(t')-\text{Cu}(t')-\text{O}-$ chains along the b direction. The vacancy of the $\text{O}(t)$ site causes the unit cell to compress slightly along a to render $a < b$. The compound $\text{TmBa}_2\text{Cu}_3\text{O}_{7-\delta}$ (Andr1) and other rare earth analogues (Lepa1) are isostructural with $\text{YBa}_2\text{Cu}_3\text{O}_{7-\delta}$.

Table VI-9 gives the bond distances and bond angles of this structure (Beech, Benoz, Borde, Cales, Coxzz, Greed, Hazen, Lepag, Siegr, Yanz2) and their temperature dependence has also been reported (Antso, Cappo).

A transmission electron microscope examination of $\text{YBa}_2\text{Cu}_3\text{O}_{7-\delta}$ in the superconducting state indicated that it is orthorhombic with the space group $Pm2m$, C_{2v}^1 and the lattice constants $a = 3.80$, $b = 3.86$, and $c = 11.55$. The a and b axes alternate across an antiphase boundary which runs parallel to the $[110]$ direction.

A yttrium-rich phase of YBaCuO was found to have the structure $Pnma$, D_{2h}^{16} with $a = 13.5 \text{ \AA}$, $b = 6.3 \text{ \AA}$, and $c = 7.6 \text{ \AA}$ (Eagle). $\text{GdBa}_2\text{Cu}_3\text{O}_{7-\delta}$ has $a = 3.909$, $b = 3.849$, and $c = 11.682 \text{ \AA}$ with the following possible space groups: $Pmmm$, D_{2h}^1 ; $Pmm2$, C_{2v}^1 ; $P222$, D_2^1 (Xuzz1). $\text{YBa}_2\text{Cu}_3\text{O}_{7-\delta}$ has also been assigned

TABLE VI-8.
with Orthorh

R-M

Y-Ba

Dy-Ba

Er-Ba

Eu-Ba

Gd-Ba

Ho-Ba

Lu-Ba

Nd-Ba

TABLE VI-8. Selected Lattice Parameters for $RM_2Cu_3O_{7-\delta}$ Type Superconductors with Orthorhombic Structure^a

R-M	δ	Lattice Parameters			ANIS	Ref.
		a (Å)	b (Å)	c (Å)		
Y-Ba	0.62	3.85	3.86	11.78	0.26	Kuboz
	0.57	3.85	3.87	11.77	0.52	Kuboz
	0.47	3.84	3.88	11.75	1.04	Kuboz
	0.28	3.8237	3.8874	11.657	1.65	Tara3
	0.19	3.8231	3.8864	11.6807	1.64	Benoz
	0.15	3.8282	3.8897	11.6944	1.59	Bonn1
	0.1	3.8591	3.9195	11.8431	1.55	Jorge
	0.1	3.83	3.89	11.7	1.55	Kuboz
	0	3.8124	3.8807	11.6303	1.75	Cappo
	0	3.825	3.886	11.660	1.58	Relle
	0	3.856	3.870	11.666	0.36	Siegr
	0	3.825	3.883	11.68	1.50	Ginle
	0	3.825	3.883	11.68	1.50	Ventu
	0	3.816	3.892	11.682	1.97	Greed
	0	3.84	3.88	11.63	1.04	Ding1
	0	3.82	3.88	11.67	1.56	Crabt
	0	3.817	3.882	11.671	1.69	Coxzz
	0	3.8271	3.8771	11.7086	1.30	Larb1
	0	3.83	3.89	11.71	1.55	Worth
Dy-Ba	0	3.828	3.886	11.66	1.50	Mapl1
	0	3.941	3.894	11.673	1.37	Yamad
Er-Ba	0.18	3.828	3.889	11.668	1.58	Tara3
	0	3.844	3.885	11.532	1.06	Kuzzz
	0	3.845	3.884	11.53	1.01	Lynnz
	0	3.813	3.874	11.62	1.59	Mapl1
	0	3.832	3.88	11.639	1.24	Yamad
Eu-Ba	0.18	3.815	3.884	11.659	1.79	Tara3
	-0.1	3.8449	3.9007	11.704	1.40	Tara3
	0	3.8152	3.8822	11.6502	1.74	Golbe
	0	3.843	3.897	11.7	1.40	Mapl1
Gd-Ba	0	3.851	3.901	11.746	1.29	Yamad
	-0.08	3.840	3.899	11.703	1.52	Tara3
	0	3.836	3.894	11.62	1.50	Mapl1
	0	3.845	3.898	11.732	1.37	Yamad
Ho-Ba	0	3.845	3.886	11.547	1.06	Kuzzz
	0	3.8253	3.8856	11.6578	1.56	Leez2
	0	3.821	3.886	11.66	1.69	Mapl1
	0	3.841	3.883	11.676	1.09	Yamad
	0.29	3.822	3.888	11.670	1.71	Tara3
Lu-Ba	0	3.835	3.886	11.531	1.32	Kuzzz
	0	3.791	3.859	11.57	1.78	Mapl1
Nd-Ba	-0.16	3.8546	3.9142	11.736	1.53	Tara3
	0	3.867	3.906	11.71	1.00	Mapl1
	0	3.873	3.902	11.761	0.75	Yamad

TABLE VI-8. (continued)

R-M	δ	Lattice Parameters			ANIS	Ref.
		a (Å)	b (Å)	c (Å)		
Sm-Ba	-0.11	3.855	3.899	11.721	1.13	Tara3
	0	3.843	3.906	11.72	1.63	Mapl1
	0	3.867	3.909	11.75	1.08	Yamad
Tm-Ba	0	3.836	3.885	11.529	1.27	Kuzzzz
	0	3.845	3.881	11.618	0.93	Yamad
	0	3.802	3.878	11.63	1.98	Mapl1
	0.35	3.810	3.882	11.656	1.87	Tara3
Yb-Ba	0.29	3.7989	3.8727	11.650	1.92	Tara3
	0	3.834	3.884	11.531	1.30	Kuzzzz
	0	3.798	3.87	11.61	1.88	Mapl1
	0	3.832	3.83	11.61	0.05	Yamad

*The table is sorted by cations and then by decreasing oxygen deficiency parameter, δ . ANSI is the anisotropy factor $100|b - a|/0.5(b + a)$ (prepared by M. M. Rigney).

TABLE VI-9. Selected Bond Distances and Angles in $\text{YBa}_2\text{Cu}_3\text{O}_7$, Where n is Number of Equivalent Bonds"

Bond	Distance (Å)	<i>n</i>	Mean (Å)
Cu(t)-O(t')	1.941	2	1.886
-O(b)	1.831	2	
Cu(m)-O(b)	2.285	1	1.943
-O(m)	1.931	2	
-O(m')	1.955	2	
Ba-O(t')	2.891	2	2.864
-O(m)	2.976	2	
-O(m')	2.963	2	
-O(b)	2.747	4	
Y-O(m)	2.404	4	
-O(m')	2.383	4	2.394
Configuration		Angle (deg)	
Cu(t)-O(t')-Cu(t)		180	
Cu(m)-O(m)-Cu(m)		163.6	
Cu(m)-O(m')-Cu(m)		164.0	

*The bond distances are averages of those reported by various investigators (Beech, Benoz, Borde, Cappel, Coxzz, Greed, Lepag, Siegr); the angles are from Coxzz.

to the orthorhombic structure, $a = 3.89$ Å and $c = 3.89$ Å.

3. Temperatur

The structure Benoz, Cappo square displac thermal vibra that there is a investigators. investigators (Antso, Cappo averages over tions in the x. We see from chain coppers the oxygens C

4. Phase Tra

The compound exhibits a second-order phase transition at $T_c = 10.5$ K. The orthorhombic phase is described by the Jorg3, Sagee phase sketch. The disordering and ordering transitions are disordered and ordered. This occurs at $T_c = 10.5$ K and randomizes the orthorhombic superlattice.

Figure VI
plane as a fun
sphere (Jorge
the fractiona
 δ in the form
pound ($T \approx$
occupancies
gen. An anoi
ducting tran

The ortho
The tetragor
above the ph
does not form
tioned in Se

to the orthorhombic space group $Pmm2$, D_{2v}^1 with $a = 3.820 \text{ \AA}$, $b = 11.688 \text{ \AA}$, and $c = 3.893 \text{ \AA}$ (Beyel), and to $Pm2m$, C_{2v}^1 .

3. Temperature Factors

The structure refinements provided temperature factors $B = 8\pi^2 \langle u^2 \rangle$ (Beech, Benoz, Cappo, Coxzz, Greed, Lepag, Siegr) which are a measure of the mean square displacement $\langle u^2 \rangle$ in \AA^2 of an atom about its equilibrium position due to thermal vibrations, and these are listed in Table VI-10. We see from the table that there is a great deal of scatter in the temperature factors reported by various investigators. This is in sharp contrast to the close agreement among these same investigators on the atom positions. The vibrations themselves are anisotropic (Antso, Cappo, Youzz), and the values listed in the table may be looked upon as averages over thermally excited normal modes. The extent of the atomic vibrations in the x , y , and z directions is indicated in Fig. VI-9 by ellipsoids (Jorge). We see from the figure that the light oxygen atoms $O(t')$ and $O(b)$ bonded to chain coppers $Cu(t)$ on the basal plane undergo larger amplitude vibrations than the oxygens $O(m)$ and $O(m')$ on the CuO_2 planes.

4. Phase Transition

The compound $YBaCuO$ is tetragonal at high temperatures and undergoes a second-order (Freil) order-disorder transition at about 700°C to the low-temperature orthorhombic phase (Bakke, Beyer, Eatou, Iwaz2, Jorge, Jorg1, Jorg2, Jorg3, Sagee, Schul, Torar, Vant2). Quenching can produce the tetragonal phase sketched on the right side of Fig. VI-9 at room temperature. The oxygens are disordered on the basal ($z = 0$) plane sites in the high-temperature phase and ordered to form chains at low temperature, as indicated on the two figures. This occurs because the two oxygen sites $O(t)$ and $O(t')$, which are equivalent and randomly occupied in the tetragonal phase, become inequivalent in the orthorhombic phase, where all of the basal plane oxygens reside on $O(t')$. A superlattice associated with this ordering has been observed (Vant2).

Figure VI-10 shows the fractional site occupancy of the oxygens in the basal plane as a function of the heating temperature of the sample in an oxygen atmosphere (Jorge). The central curve in the orthorhombic region gives the mean of the fractional occupancies of the a and b sites. This curve also gives the value of δ in the formula $YBa_2Cu_3O_{7-\delta}$. One should note that the low-temperature compound ($T \approx 25^\circ\text{C}$) of Fig. VI-10 corresponds to the formula $YBa_2Cu_3O_{6.9}$. Site occupancies were also obtained for heating in different partial pressures of oxygen. An anomaly found in the orthorhombic distortion of YBa^* at the superconducting transition (Hornz) was interpreted as evidence for anisotropic pairing.

The orthorhombic 123 structure is the superconducting phase of $YBaCuO$. The tetragonal phase can be obtained at room temperature by quenching from above the phase transition, and it is found to be semiconducting. Ordinarily it does not form a superconductor (Chen2, Kwok2), but some exceptions are mentioned in Section VI-F.

Ref.

Tara3
Mapl1
Yamad
Kuzzz
Yamad
Mapl1
Tara3
Tara3
Kuzzz
Mapl1
Yamad

h, δ . ANSI is the

Mean (\AA)

1.886

1.943

2.864

2.394

re n is

h, Benoz, Borde,

TABLE VI-10. Temperature Factors $B = 8\pi^2 \langle u^2 \rangle$ for Mean Square Displacements $\langle u^2 \rangle$ of Atoms of $\text{YBa}_2\text{Cu}_3\text{O}_7$ About Their Equilibrium Positions^a

Groups	Beech	Benoz	Cappo	Coxzz	Greed	Jorge	Lepag	Siegr
CuO ₂	O(t)	—	—	1.6	—	—	—	2.32
	Cu(t)	0.55	0.38	0.2	0.69	1.4	0.9	1.10
	O(t')	1.73	2.4	1.6	0.59	—	4.2	2.00
BaO	O(b)	0.78	0.93	0.5	1.32	—	1.6	1.30
	Ba	0.65	0.59	0.4	0.78	1.7	0.51	0.84
	Cu(m)	0.49	0.51	0.3	0.81	1.50	0.5	0.67
CuO ₂	O(m')	0.55	0.31	0.4	0.38	1.3	0.2	1.20
	O(m)	0.57	0.11	0.5	0.36	1.6	0.2	0.40
	Y	0.56	0.58	0.2	0.60	1.4	0.7	0.53
CuO ₂	O(m)	0.57	0.11	0.5	0.36	1.6	0.2	0.40
	O(m')	0.55	0.31	0.4	0.38	1.3	0.2	1.20
	Cu(m)	0.49	0.51	0.3	0.81	1.50	0.5	0.67
BaO	Ba	0.65	0.59	0.4	0.78	1.7	0.51	0.84
	O(b)	0.78	0.93	0.5	1.32	—	1.6	1.30
	O(t)	—	—	1.6	—	—	—	2.32
CuO ₂	Cu(t)	0.55	0.38	0.2	0.69	1.4	0.9	1.10
	O(t')	1.73	2.4	1.6	0.59	—	4.2	2.00

^aThe results of several investigations are shown; some (Antso, Borde, Cappo, Jorge) give anisotropic values.

Fig. VI-10. D (bottom) sites (right) on the c the two sites.

5. Oxygen-S

Various worl eral of them : convention, ; the letters t and m' for t the barium l

6. Generatic

The YBaCu(prototype for above the of Column 6 of erate the YB replaced by moved, as ir removed oxy

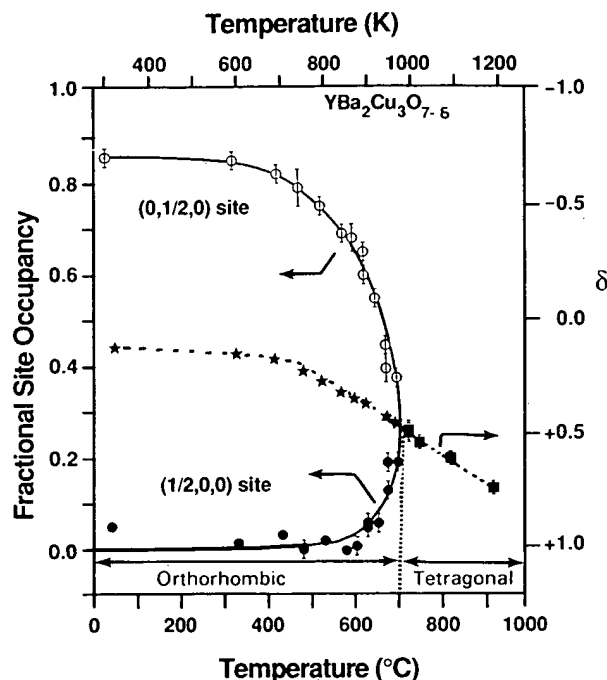


Fig. VI-10. Dependences of the fractional occupancies of the $(0, \frac{1}{2}, 0)$ (top) and $(\frac{1}{2}, 0, 0)$ (bottom) sites (scale on left) and of the oxygen content parameter δ (center curve, scale on right) on the quench temperature. This latter curve is the average of the occupancies of the two sites. (Adapted from Jorge.)

5. Oxygen-Site Nomenclature

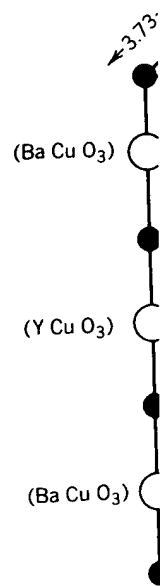
Various workers use different numbering schemes for the oxygen sites, and several of them are compared in Table VI-11. We have adopted the more mnemonic convention, given in column 3 of the table and illustrated in Fig. VI-9, of using the letters t and t' for top (and equivalent bottom) copper oxide layer, and m and m' for the median copper oxide layers, with $O(b)$ denoting the oxygen on the barium level.

6. Generation of YBaCuO Structure

The YBaCuO tetragonal structure may be visualized as being derived from three prototype fcc oxygen unit cells of the type illustrated on Fig. VI-1, stacked one above the other along the z or c axis, as shown in the center of Fig. VI-11. Column 6 of Table VI-6 gives the z parameter values for this ideal case. To generate the YBaCuO tetragonal unit cell the barium centered in the middle cube is replaced by yttrium, and the oxygens on the edges of this middle cube are removed, as indicated on the left side of Fig. VI-11. To take up the space of the removed oxygens and that arising from the smaller size of yttrium, the center

TABLE VI-11. Notations Used for Atoms in $\text{YBa}_2\text{Cu}_3\text{O}_{7-\delta}$

Group	Plane	Present Work ^a	Site (Pmm)	Beech, Cappel, Coxzz, Siegr, Yauzz, Youzz	Benoz, Hazen, Jorge	Antso	Borde ^b	Greedy	Lepag
CuO	Top plane	O(t)	1e	[O(5)]	—	—	—	—	—
		Cu(t)	1a	Cu(1)	Cu(1)	Cu(1)	Cu(1)	Cu(1)	Cu(1)
		O(t')	1b	O(4)	O(1)	O(1)	O(1)	O(1)	O(1)
BaO	Upper barium plane	O(b)	2q	O(1)	O(4)	O(2)	O(1)	O(2)	O(3)
		Ba	2t	Ba	Ba	Ba	Ba	Ba	Ba
		Cu(m)	2q	Cu(2)	Cu(2)	Cu(2)	Cu(2)	Cu(2)	Cu(2)
CuO ₂	Upper median plane	O(m')	2r	O(3)	O(3)	O(3)	O(2)	O(4)	O(2)
		O(m)	2s	O(2)	O(2)	O(4)	O(2)	O(3)	O(2)
		Y	1h	Y	Y	Y	Y	Y	Y
CuO ₂	Lower median plane	O(m)	2s	O(2)	O(2)	O(4)	O(2)	O(3)	O(2)
		O(m')	2r	O(3)	O(3)	O(3)	O(2)	O(4)	O(2)
		Cu(m)	2q	Cu(2)	Cu(2)	Cu(2)	Cu(2)	Cu(2)	Cu(2)
BaO	Lower barium plane	Ba	2t	Ba	Ba	Ba	Ba	Ba	Ba
		O(b)	2q	O(1)	O(4)	O(2)	O(1)	O(2)	O(3)
		O(t)	1b	[O(5)]	—	—	—	—	—
CuO	Bottom plane	Cu(t)	1a	Cu(1)	Cu(1)	Cu(1)	Cu(1)	Cu(1)	Cu(1)
		O(t')	1e	O(4)	O(1)	O(1)	—	O(1)	O(1)

^aOxygen sites O(t) and O(m) are along the shorter a axis ($x = \frac{1}{2}, y = 0$).^b $\text{Y}_{0.3}\text{Ba}_{2.1}\text{Cu}_3\text{O}_6$.Fig. VI-11. G stacked BaCuO_3 level where Y

cube is com
moved along
dinated for
Cu-O distan
shown in Fig
pyramidal c
1.94 Å in th
 $\delta = 0$ comp
the left side

7. Layering

In Section V
conductors.
Fig. VI-13,
threefold la
much close
indicated in
median lay
between th

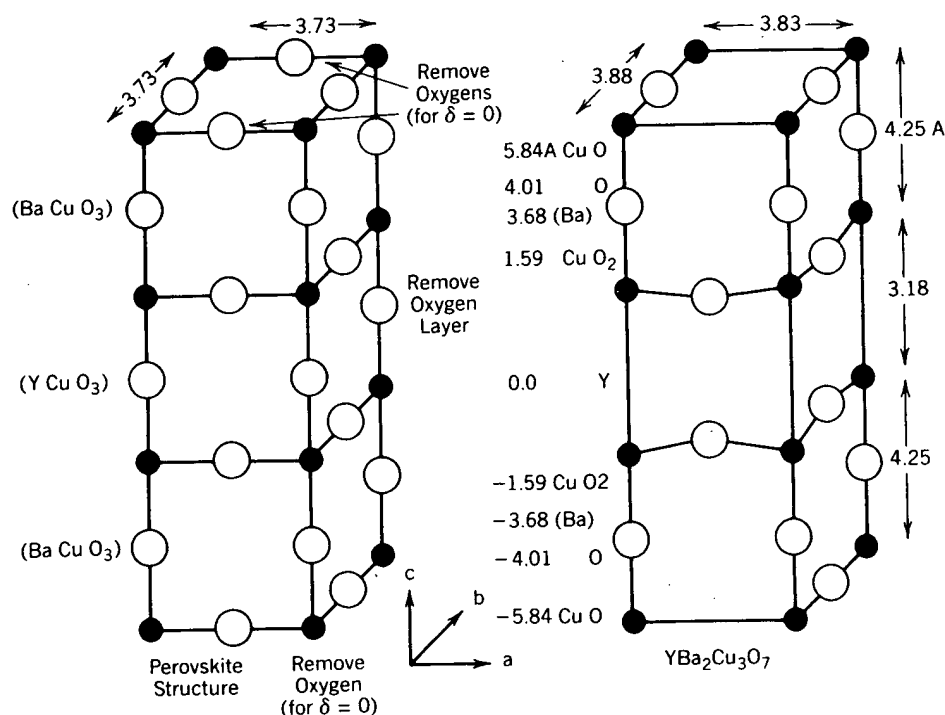


Fig. VI-11. Generation of the yttrium-barium-copper oxide unit cell (right) from three stacked BaCuO_3 perovskite unit cells (left) by the removal of the oxygens on the yttrium level where Y replaces Ba.

cube is compressed along the c direction. Finally, the vertical edge oxygens are moved along c toward the apical Cu(t) ions. This copper ion Cu(t) is sixfold coordinated for $\text{YBa}_2\text{Cu}_3\text{O}_8$ and square-planar coordinated for $\text{YBa}_2\text{Cu}_3\text{O}_7$ with Cu-O distances of 1.94 \AA in the basal xy plane and 1.83 \AA vertically along c , as shown in Fig. VI-12. The two other coppers, Cu(m) and Cu(m'), exhibit fivefold pyramidal coordination, as indicated in Fig. VI-14, with Cu-O spacings of 1.94 \AA in the basal plane and 2.29 \AA vertically. One should note that the final $\delta = 0$ compound only differs in composition from the prototype perovskite on the left side of Fig. VI-11 by the deficiency of two oxygens.

7. Layering Scheme of YBaCuO

In Section VI-E-6 we discussed the CuO_2 layering scheme of the LaSrCuO superconductors. The layering scheme of the YBaCuO case, which is illustrated in Fig. VI-13, is somewhat more complicated than the LaSrCuO case. There is a threefold layering sequence with the two median planes adjacent to the yttrium much closer together (3.18 \AA) than they are to the basal plane (4.25 \AA), as indicated in the figure. The basal plane copper ions Cu(t) are coupled to the median layer coppers Cu(m) through oxygens, and such coupling does not exist between the two median planes. The basal plane coppers and oxygens are in

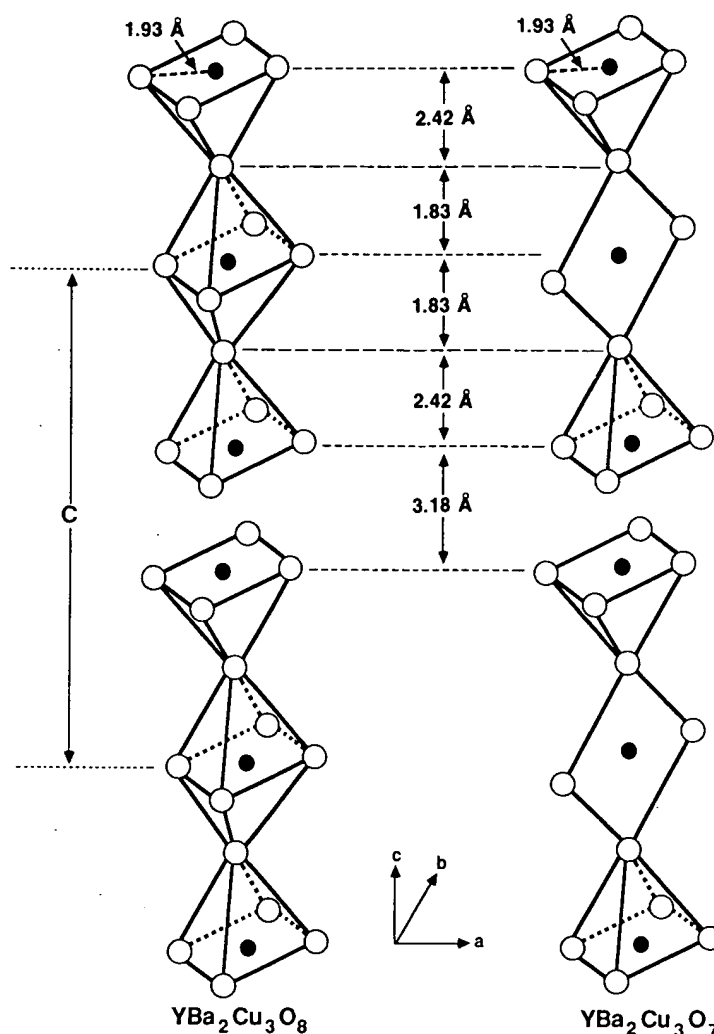


Fig. VI-12. Ordering of the YBaCuO copper atoms and their associated oxygen nearest neighbors along the c axis. The arrangement is a stacking of pyramid-octahedron-inverted-pyramid groups in the tetragonal structure (left) and of pyramid-square-planar-inverted-pyramid groups in the orthorhombic structure (right).

special sites so the plane is perfectly flat, as shown. In contrast to this the median plane coppers and oxygens are both in general sites with slightly different z parameters, so the median planes have a puckered appearance with a thickness of about 0.23 \AA , as indicated in Figs. VI-9 and VI-13.

The case illustrated in Fig. VI-13 corresponds to $\text{YBa}_2\text{Cu}_3\text{O}_{7-\delta}$ with $\delta = 0$, so the oxygen sites along the a direction of the basal plane are all empty and those along the b direction are all occupied. This produces Cu-O-Cu-O chains along the b direction, as shown in the figure. The missing oxygens cause the coppers to move slightly closer together along a , thereby inducing the orthorhombic distortion with $a < b$.

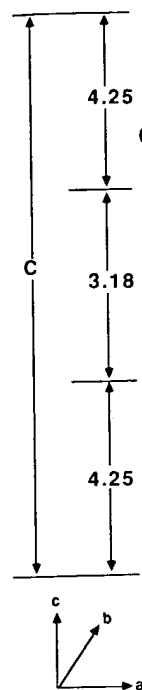


Fig. VI-13. Layer structure of YBaCuO. The layers are indicated by the arrows.

tion with $a < b$ occupy the vacant sites.

8. YBaCuO I

Since yttrium is a trivalent ion, the charge on copper is trivial. For the high- T_c superconductors, the copper is in a strong tendency to be in a $+2$ state. In $\text{YBa}_2\text{Cu}_3\text{O}_7$, the oxygen atoms are ordered and the copper atoms are in a $+2$ state. The case corresponds to the $+2$ and $+1$ states of copper, which are discussed at great length in the literature.

An extra layer of copper atoms (Zandl) consists of

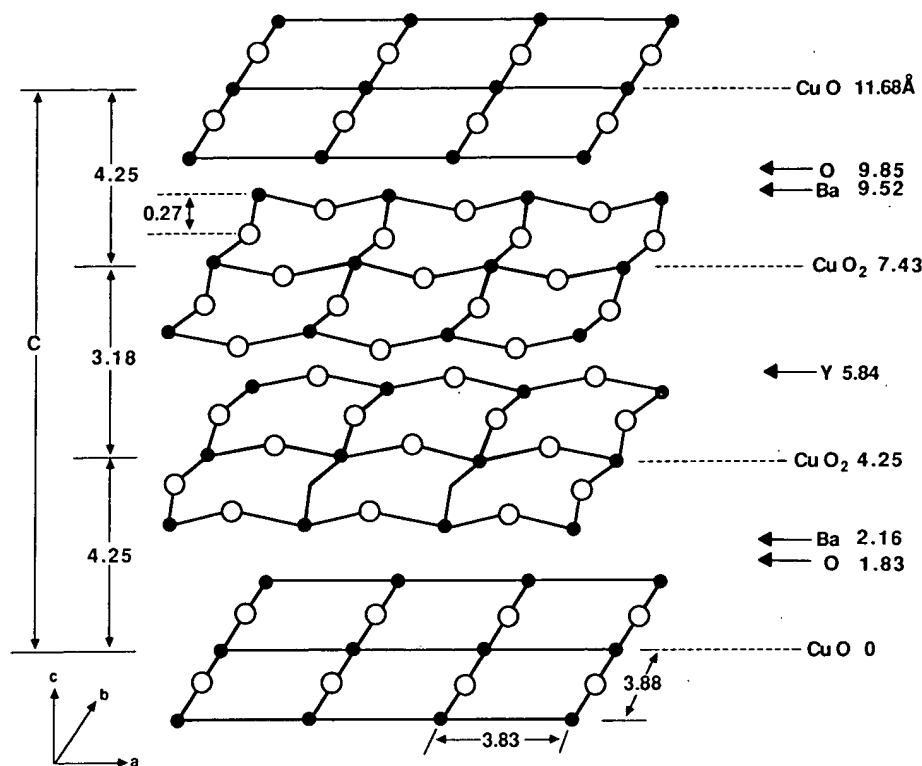


Fig. VI-13. Layering scheme of the YBaCuO superconducting (orthorhombic) structure. The layers are perpendicular to the c axis. The extent of puckering of the median CuO_2 layers is indicated.

tion with $a < b$. When the oxygen content increases ($\delta < 0$), oxygens begin to occupy the vacant sites along a .

8. YBaCuO Defect Structures

Since yttrium has a charge of +3, barium is +2, and oxygen is -2, it follows that for the hypothetical compound $\text{YBa}_2\text{Cu}_3\text{O}_8$ which has $\delta = -1$, all of the copper is trivalent (+3). This compound cannot be prepared because of the strong tendency toward oxygen deficiency. We have seen that the compound $\text{YBa}_2\text{Cu}_3\text{O}_7$ with $\delta = 0$ has all of its oxygen loss in the basal plane where linear O-Cu-O coordination replaces square planar CuO_4 . The oxygen vacancies are ordered and hence the copper ions form $(\text{Cu}-\text{O})_n$ chains in this plane. This $\delta = 0$ case corresponds to an average copper charge of 2.33, which suggests a mixture of +2 and +3 copper valence states. Samples with $\delta = 0.5$ (e.g., Hazen) have an average copper charge of 2.0. This subject of copper valence has been discussed at greater length in Section III-J.

An extra layer of yttrium atoms (Ourma) or an extra or double CuO plane (Zand1) constitute common planar defects in the YBaCuO structure. The pres-

ence of such a planar defect may be visualized as enlarging a unit cell on the right-hand side of Fig. VI-11 from, in the yttrium case, a threefold Ba, Y, Ba sequence to a fourfold Ba, Y, Ba, Y sequence, with this sequence continuing indefinitely in the horizontal direction. Other unit cells are left unchanged. Square planar CuO_2 has been found in the structures of $(\text{Y}_{1-x}\text{Ba}_x)_3\text{Cu}_2\text{O}_6$ and $(\text{Y}_{1-x}\text{Ba}_x)_3\text{Cu}_2\text{O}_7$ (Kitaz).

G. OTHER LaSrCuO AND YBaCuO STRUCTURES

The system $\text{La}(\text{Ba}_{1-x}\text{La}_x)_2\text{Cu}_3\text{O}_{7+\delta}$ has the region of solubility $0.125 < x < 0.25$. These compounds are disordered isomorphs of the orthorhombic $\text{YBa}_2\text{Cu}_3\text{O}_7$ structure (Segre). The highest $T_c = 60$ K occurs for $x = 0.065$ and $x = 0$, the latter stoichiometric compound $\text{LaBa}_2\text{Cu}_3\text{O}_{7-\delta}$ being outside the range of solubility. The compounds $\text{La}_2\text{SrCu}_2\text{O}_{6.2}$, $\text{La}_4\text{BaCu}_5\text{O}_{13}$, and $\text{La}_5\text{SrCu}_6\text{O}_{15}$ are not superconducting (Torri).

Studies of related superconducting compounds such as $(\text{La}_{1.6}\text{Ba}_{0.4})\text{CuO}_{4-\delta}$, $(\text{La}_{0.8}\text{Ba}_{0.2})\text{CuO}_{4-\delta}$, and $(\text{Y}_{0.8}\text{Ba}_{0.2})\text{CuO}_{4-\delta}$ (Kirs1, Kirs2), and $(\text{Y}_{0.4}\text{Ba}_{0.6})\text{CuO}_3$ (Luo2) have been reported. See also Bedn4.

The green semiconducting phase Y_2BaCuO_5 which is often found admixed with superconducting $\text{YBa}_2\text{Cu}_3\text{O}_7$ is orthorhombic and was assigned to the space group $Pbnm$, D_{2h}^{16} or $Pna2_1$, C_{2v}^9 (Hazen, Kitan, Mansf, Mich2, Rao2, Rossz) with $a = 7.1$ Å, $b = 12.2$ Å, and $c = 5.6$ Å.

The compound La_2CuO_4 was identified as the first member ($n = 1$) of the homologous series of composition $\text{R}_{n+1}\text{M}_n\text{O}_{3n+1}$ with $\text{R} = \text{La}$ and $\text{M} = \text{Cu}$ in the present case (Davie). Several members of the series were prepared with n in the range from 1 to 6, and their crystallography consisted of slabs of $(\text{LaCuO}_3)_n$ groups containing CuO_6 octahedra with a perovskite-type structure separated by layers of LaO with the La and O atoms in an NaCl -type structure, as shown on Fig. VI-14. The perovskite LaCuO_3 , which plays the role of the limiting structure of $\text{La}_{n+1}\text{Cu}_n\text{O}_{3n+1}$ as $n \rightarrow \infty$, is shown for comparison.

Other oxide types have also been mentioned in the literature, such as the possible lower symmetry space groups of the R_2MO_4 structure arising from rigid octahedral tiltings at phase transitions (Hatch).

H. BISMUTH-STRONTIUM-CALCIUM-COPPER OXIDE

Early in 1988 two new superconducting systems were discovered which have transition temperatures considerably above those attainable with the YBaCuO compounds, namely, the bismuth- (Chuz2, Maeda, Zand2) and the thallium- (Gao2, Hazel, Sheng, Shen1) based materials. In this section we will discuss the structure of BiSrCaCuO , and in the next we will treat TlBaCaCuO .

The 2212 compound $\text{Bi}_2(\text{Sr}, \text{Ca})_3\text{Cu}_2\text{O}_{8+\delta}$ crystallizes in the same tetragonal space group $I4/mmm$, D_{4h}^{17} as La_2CuO_4 with two formula units per unit cell and

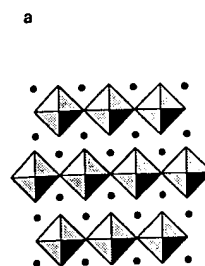


Fig. VI-14. Ideal $\text{La}_{n+1}\text{Cu}_n\text{O}_{3n+1}$ structure. The squares are CuO_6 octahedra, the gonal cell is projected.

the lattice parameter a is the same as the c axis of the LaCuO_3 structure.

where the atom positions are those for site (1) and (2) of the following atom

(8g)

Table VI-12 gives the atomic positions and have been reported.

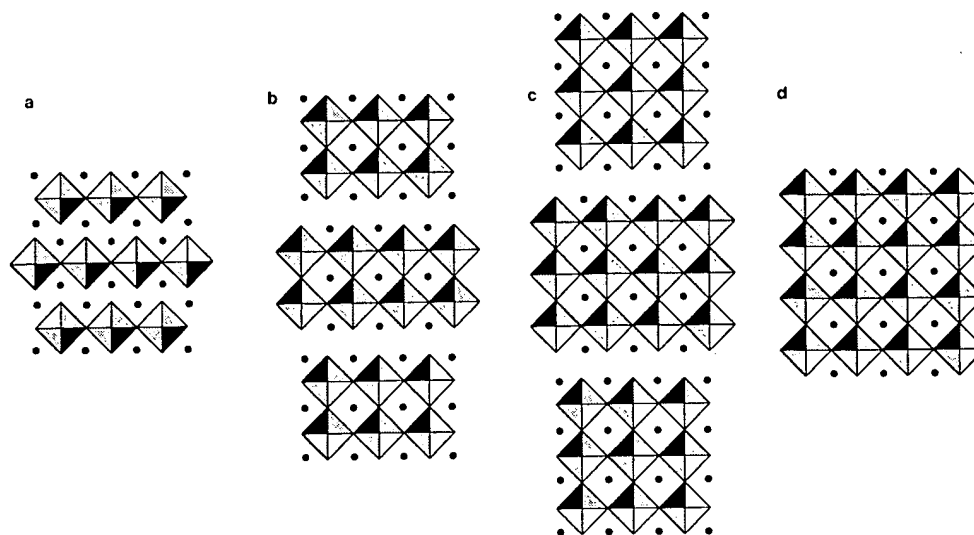


Fig. VI-14. Idealized representations of the structures of the series of compounds $\text{La}_{n+1}\text{Cu}_n\text{O}_{3n+1}$ with (a) $n = 1$, (b) $n = 2$, (c) $n = 3$, and (d) LaCuO_3 ($n = \infty$). The squares are CuO_6 octahedra and the solid circles denote La atoms. In (a)–(c) the tetragonal cell is projected down $[010]$ and the c axis is vertical (Davie).

the lattice parameters $a = 3.817 \text{ \AA}$, $c = 30.6 \text{ \AA}$ (Tara9). The parameters for the atoms are:

Ca	(2a)		
Sr	(4e)	$u = 0.1097$	
Bi	(4e)	$u = 0.3022$	87% occupancy
Bi	(4e)	$u = 0.2681$	13% occupancy
Cu	(4e)	$u = 0.4456$	
O(1)	(8g)	$u = 0.446$	
O(2)	(4e)	$u = 0.375$	
O(3)	(4e)	$u = 0.205$	
O(4)	(4d)		6.5% occupancy

(VI-12)

where the atom positions for sites (2a) and (4e) are given above in Eq. VI-6, those for site (4d) are given by Eq. VI-7, and the remaining site (8g) has the following atom positions:

$$(8g) \quad 0, \frac{1}{2}, u; 0, \frac{1}{2}, -u; \frac{1}{2}, 0, u; \frac{1}{2}, 0, -u; \frac{1}{2}, 0, u + \frac{1}{2}; \frac{1}{2}, 0, -u + \frac{1}{2}; 0, \frac{1}{2}, u + \frac{1}{2}; 0, \frac{1}{2}, -u + \frac{1}{2} \quad (\text{VI-13})$$

Table VI-12 gives more details on the atom positions. Superlattice structures have been reported along a and b (Iqba6).

TABLE VI-12. Atom Positions of $\text{Bi}_2\text{Sr}_2\text{CaCu}_2\text{O}_{8+\delta}$ Structure with Two Formula Units per Unit Cell^a

Complex	Vertical Position	Atom	Site	x	y	z
Ca	30.6	Ca	2a	0	0	1.0
O ₂ Cu	29.0	O(1)	8g	0	$\frac{1}{2}$	0.9460
	29.0	O(1)	8g	$\frac{1}{2}$	0	0.9460
	28.9	Cu	4e	$\frac{1}{2}$	$\frac{1}{2}$	0.9456
SrO	27.2	Sr	4e	0	0	0.8903
	26.8	O(2)	4e	$\frac{1}{2}$	$\frac{1}{2}$	0.8750
OBi	24.5	Bi	4e	$\frac{1}{2}$	$\frac{1}{2}$	0.8022
	24.3	O(3)	4e	0	0	0.7950
BiO ₂	23.5	Bi'	4e	$\frac{1}{2}$	$\frac{1}{2}$	0.7681
	23.0	O(4)	2d	0	$\frac{1}{2}$	$\frac{3}{4}$
	23.0	O(4)	2d	$\frac{1}{2}$	0	$\frac{3}{4}$
	22.4	Bi'	4e	0	0	0.7319
BiO	21.6	O(3)	4e	$\frac{1}{2}$	$\frac{1}{2}$	0.7050
	21.4	Bi	4e	0	0	0.6978
OSr	19.1	O(2)	4e	0	0	0.6250
	18.7	Sr	4e	$\frac{1}{2}$	$\frac{1}{2}$	0.6097
CuO ₂	17.0	Cu	4e	0	0	0.554
	17.0	O(1)	8g	0	$\frac{1}{2}$	0.554
	17.0	O(1)	8g	$\frac{1}{2}$	0	0.554
Ca	15.3	Ca	2a	$\frac{1}{2}$	$\frac{1}{2}$	$\frac{1}{2}$
	13.6	O(1)	8g	$\frac{1}{2}$	0	0.4460
	13.6	O(1)	8g	0	$\frac{1}{2}$	0.4460
	13.6	Cu	4e	0	0	0.4456
OSr	11.9	Sr	4e	$\frac{1}{2}$	$\frac{1}{2}$	0.3903
	11.5	O(2)	4e	0	0	0.3750
BiO	9.25	Bi	4e	0	0	0.3022
	9.03	O(3)	4e	$\frac{1}{2}$	$\frac{1}{2}$	0.2950
BiO ₂	8.20	Bi'	4e	0	0	0.2681
	7.65	O(4)	2d	$\frac{1}{2}$	0	$\frac{1}{4}$
	7.65	O(4)	2d	0	$\frac{1}{2}$	$\frac{1}{4}$
	7.10	Bi'	4e	$\frac{1}{2}$	$\frac{1}{2}$	0.2319
OBi	6.27	O(3)	4e	0	0	0.2050
	6.05	Bi	4e	$\frac{1}{2}$	$\frac{1}{2}$	0.1978
SrO	3.83	O(2)	4e	$\frac{1}{2}$	$\frac{1}{2}$	0.1250
	3.36	Sr	4e	0	0	0.1097
O ₂ Cu	1.66	Cu	4e	$\frac{1}{2}$	$\frac{1}{2}$	0.0544
	1.65	O(1)	8g	$\frac{1}{2}$	0	0.0540
	1.65	O(1)	8g	0	$\frac{1}{2}$	0.0540
Ca	0	Ca	2a	0	0	0

^aThe space group is $I4/mmm$, D_{4h}^{17} . The unit cell dimensions are $a = 3.817 \text{ \AA}$, $c = 30.6 \text{ \AA}$ (Tara9).TABLE VI-13. Atoms in $I4/mmm$, D_{4h}^{17} with

Complex	Ve
Ca	2
O ₂ Cu	2
	2
	2
BaO	2
	2
OTl	2
	2
TlO	2
	2
OBa	2
	2
CuO ₂	2
	2
Ca	2
CuO ₂	2
	2
OBa	2
	2
TlO	2
	2
OTl	2
	2
BaO	2
	2
O ₂ Cu	2
	2
Ca	2

^aThe unit cell dimensions are

I. THALLIUM

The compound $I4/mmm$, D_{4h}^{17} units per unit (Subra). The a

TABLE VI-13. Atom Positions of $\text{Ti}_2\text{Ba}_2\text{CaCu}_2\text{O}_8$ Structure Belonging to Space Group $I4/mmm$, D_{4h}^{17} with Two Formula Units per Unit Cell^a

Complex	Vertical Position	Atom	Site	x	y	z
Ca	29.32	Ca	2a	0	0	1.0
O ₂ Cu	27.76	O(1)	8g	0	$\frac{1}{2}$	0.9469
	27.76	O(1)	8g	$\frac{1}{2}$	0	0.9469
	27.74	Cu	4e	$\frac{1}{2}$	$\frac{1}{2}$	0.946
BaO	25.75	Ba	4e	0	0	0.8782
	25.04	O(2)	4e	$\frac{1}{2}$	$\frac{1}{2}$	0.8539
OTl	23.06	Tl	4e	$\frac{1}{2}$	$\frac{1}{2}$	0.7864
	22.91	O(3)	16n	0.104	0	0.7815
TlO	21.07	O(3)	16n	0.604	$\frac{1}{2}$	0.7185
	20.92	Tl	4e	0	0	0.7136
OBa	18.94	O(2)	4e	0	0	0.6461
	18.23	Ba	4e	$\frac{1}{2}$	$\frac{1}{2}$	0.6218
CuO ₂	16.24	Cu	4e	0	0	0.5540
	16.22	O(1)	8g	0	$\frac{1}{2}$	0.5531
	16.22	O(1)	8g	$\frac{1}{2}$	0	0.5531
Ca	14.66	Ca	2a	$\frac{1}{2}$	$\frac{1}{2}$	$\frac{1}{2}$
CuO ₂	13.10	O(1)	8g	$\frac{1}{2}$	0	0.4469
	13.10	O(1)	8g	0	$\frac{1}{2}$	0.4469
	13.08	Cu	4e	0	0	0.4460
OBa	11.09	Ba	4e	$\frac{1}{2}$	$\frac{1}{2}$	0.3782
	10.38	O(2)	4e	0	0	0.3539
TlO	8.40	Tl	4e	0	0	0.2864
	8.25	O(3)	16n	0.604	$\frac{1}{2}$	0.2815
OTl	6.41	O(3)	16n	0.104	0	0.2185
	6.26	Tl	4e	$\frac{1}{2}$	$\frac{1}{2}$	0.2136
BaO	4.28	O(2)	4e	$\frac{1}{2}$	$\frac{1}{2}$	0.1461
	3.57	Ba	4e	0	0	0.1218
O ₂ Cu	1.58	Cu	4e	$\frac{1}{2}$	$\frac{1}{2}$	0.0540
	1.56	O(1)	8g	$\frac{1}{2}$	0	0.0531
	1.56	O(1)	8g	0	$\frac{1}{2}$	0.0531
Ca	0	Ca	2a	0	0	0

^aThe unit cell dimensions are $a = 3.8550 \text{ \AA}$, $c = 29.318 \text{ \AA}$ (Subra).

I. THALLIUM-BARIUM-CALCIUM-COPPER OXIDE

The compound $\text{Ti}_2\text{Ba}_2\text{CaCu}_2\text{O}_8$ crystallizes in the same tetragonal space group $I4/mmm$, D_{4h}^{17} as the bismuth compound described above, with two formula units per unit cell and the lattice parameters $a = 3.8550 \text{ \AA}$, $c = 29.318 \text{ \AA}$ (Subra). The atoms are at the following sites:

Formula

v	z
0	1.0
$\frac{1}{2}$	0.9460
0	0.9460
$\frac{1}{2}$	0.9456
0	0.8903
$\frac{1}{2}$	0.8750
$\frac{1}{2}$	0.8022
0	0.7950
$\frac{1}{2}$	0.7681
$\frac{1}{2}$	$\frac{3}{4}$
0	$\frac{3}{4}$
0	0.7319
$\frac{1}{2}$	0.7050
0	0.6978
0	0.6250
$\frac{1}{2}$	0.6097
0	0.554
$\frac{1}{2}$	0.554
0	0.554
$\frac{1}{2}$	$\frac{1}{2}$
0	0.4460
$\frac{1}{2}$	0.4460
0	0.4456
$\frac{1}{2}$	0.3903
0	0.3750
0	0.3022
$\frac{1}{2}$	0.2950
0	0.2681
0	$\frac{1}{4}$
$\frac{1}{2}$	$\frac{1}{4}$
$\frac{1}{2}$	0.2319
0	0.2050
$\frac{1}{2}$	0.1978
$\frac{1}{2}$	0.1250
0	0.1097
$\frac{1}{2}$	0.0544
0	0.0540
$\frac{1}{2}$	0.0540
0	0

 $= 30.6 \text{ \AA}$ (Tara9).

J. WATSON RESEARCH CENTER LIBRARY

Ca	(2a)		
Tl	(4e)	$u = 0.21359$	
Ba	(4e)	$u = 0.12179$	
Cu	(4e)	$u = 0.0540$	(VI-14)
O(1)	(8g)	$u = 0.0531$	
O(2)	(4e)	$u = 0.1461$	
O(3)	(16n)	$v = 0.604, \quad u = 0.2815$	

where the atom positions for sites (2a), (4e), and (8g) are the same as in the previous section. The remaining $\frac{1}{4}$ occupied site (16n) has two parameters v and u , and the following possible atom positions:

$$\begin{aligned}
 (16n) \quad & 0, v, u; 0, v, -u; 0, -v, u; 0, -v, -u; \frac{1}{2}, v + \frac{1}{2}, u + \frac{1}{2}; \\
 & \frac{1}{2}, v + \frac{1}{2}, -u + \frac{1}{2}; 0, -v + \frac{1}{2}, u + \frac{1}{2}; 0, -v + \frac{1}{2}, -u + \frac{1}{2} \\
 & v, 0, u; v, 0, -u; -v, 0, u; -v, 0, -u; v + \frac{1}{2}, \frac{1}{2}, u + \frac{1}{2}; \\
 & v + \frac{1}{2}, \frac{1}{2}, -u + \frac{1}{2}; -v + \frac{1}{2}, \frac{1}{2}, u + \frac{1}{2}; -v + \frac{1}{2}, \frac{1}{2}, -u + \frac{1}{2}
 \end{aligned} \quad (VI-15)$$

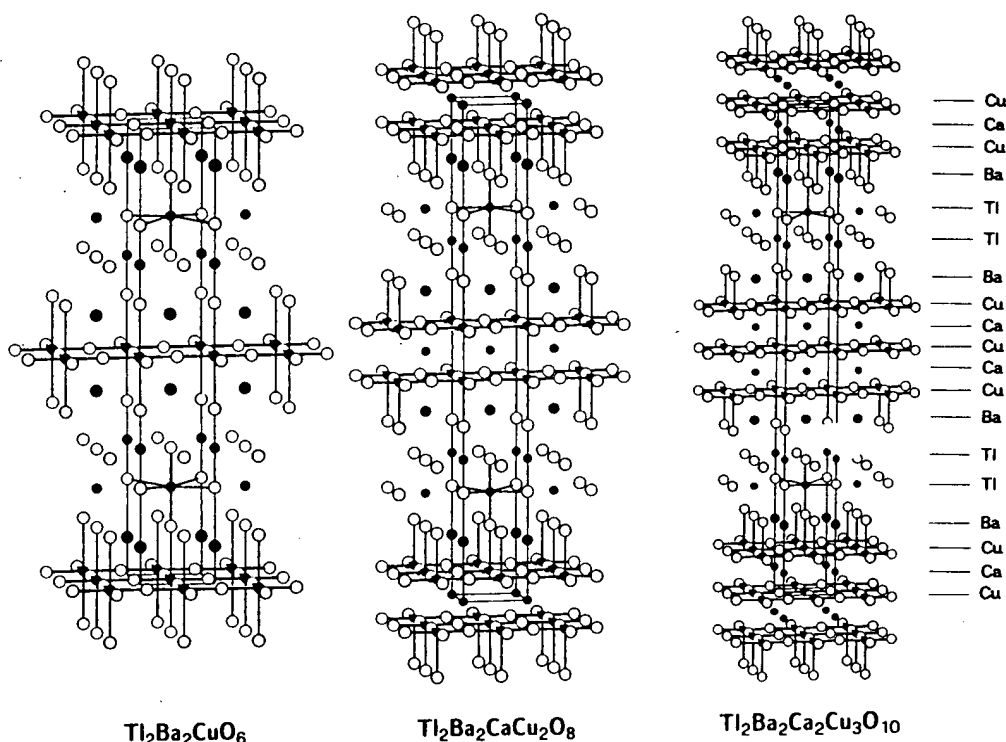


Fig. VI-15. Tetragonal unit cells of three thallium-copper oxide superconductors, $\text{Tl}_2\text{Ba}_2\text{Ca}_n\text{Cu}_{n+1}\text{O}_{6+2n}$ with, from left to right, $n = 0, 1, 2$. Metal atoms are shaded and Cu-O bonds are shown (Tora2).

Table VI-13 gives a sketch of the structure.

J. SITE SYMMETRY

Some experimental spectroscopy, symmetry of partial symmetries at These symmetries for point group

TABLE VI-14.
(with 100% stoichiometry)

Space Group

$Pm\bar{3}m, O_h^1$

$Amm2, C_{2v}^{14}$

$I4/mmm, D_{4h}^{17}$

$Fmmm, D_{2h}^{23}$

$P4/mmm, D_{4h}^1$

Table VI-13 gives more details on the atom positions and Fig. VI-15 presents a sketch of the structure.

(VI-14)

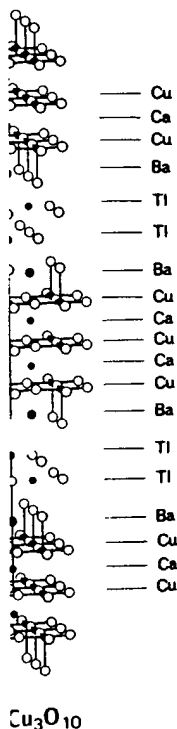
J. SITE SYMMETRIES

Some experiments such as electron spin resonance of transition ions, optical spectroscopy, and infrared spectroscopy provide data that depend upon the symmetry of particular lattice sites. Table VI-14 lists for reference purposes the site symmetries at all of the lattice sites in the various structures mentioned above. These symmetries are given in both the International and Schoenflies notations for point groups.

(VI-15)

TABLE VI-14. Point Symmetries at Lattice Sites of Various Compounds (with 100% stoichiometry)^a

Space Group	Site	Atom	Point Symmetry	
<i>Cubic Perovskite BaTiO₃</i>				
<i>Pm3m</i> , <i>O</i> _h ¹	(1a)	Ba	<i>m3m</i>	<i>O</i> _h
	(1b)	Ti	<i>m3m</i>	<i>O</i> _h
	(3c)	O	<i>4/mmm</i>	<i>D</i> _{4h}
<i>Orthorhombic Perovskite BaTiO₃</i>				
<i>Amm2</i> , <i>C</i> _{2v} ¹⁴	(2a)	Ba,O(1)	<i>mm</i>	<i>C</i> _{2v}
	(2b)	Ti	<i>mm</i>	<i>C</i> _{2v}
	(4e)	O(2)	<i>m</i>	<i>C</i> _s
<i>Tetragonal La₂CuO₄</i>				
<i>I4/mmm</i> , <i>D</i> _{4h} ¹⁷	(2a)	Cu	<i>4/mmm</i>	<i>D</i> _{4h}
	(4c)	O(1)	<i>mmm</i>	<i>D</i> _{2h}
	(4d)	O(2) (alt.str.)	<i>4m2</i>	<i>D</i> _{2d}
	(4e)	La,O(2)	<i>4mm</i>	<i>C</i> _{4v}
<i>Orthorhombic La₂CuO₄ (Longo)</i>				
<i>Fmmm</i> , <i>D</i> _{2h} ²³	(4a)	Cu	<i>mmm</i>	<i>D</i> _{2h}
	(8e)	O(1)	<i>2/m</i>	<i>C</i> _{2h}
	(8i)	La,O(2)	<i>mm</i>	<i>C</i> _{2v}
<i>Tetragonal YBa₂Cu₃O₈ (Borde, Jorge)</i>				
<i>P4/mmm</i> , <i>D</i> _{4h} ¹	(1a)	Cu(t)	<i>4/mmm</i>	<i>D</i> _{4h}
	(1d)	Y	<i>4/mmm</i>	<i>D</i> _{4h}
	(2f)	O(t)	<i>mmm</i>	<i>D</i> _{2h}
	(2g)	Cu(m), O(b)	<i>4mm</i>	<i>C</i> _{4v}
	(2h)	Ba	<i>4mm</i>	<i>C</i> _{4v}
	(4i)	O(m) = O(m')	<i>mm</i>	<i>C</i> _{2v}



perconductors, are shaded and

J. J. WATSON RESEARCH CENTER

TABLE VI-14. (continued)

Space Group	Site	Atom	Point Symmetry	
<i>Tetragonal YBa₂Cu₃O₈ (Hazen)</i>				
$\bar{P}4m2, D_{2d}^5$	(1a)	Cu(t)	$\bar{4}2m$	D_{2d}
	(1c)	Y	$\bar{4}2m$	D_{2d}
	(2e)	Cu(m),O(b)	mm	C_{2v}
	(2f)	Ba	mm	C_{2v}
	(2g)	O(t),O(m),O(m')	mm	C_{2v}
<i>Orthorhombic YBa₂Cu₃O₈^b</i>				
$Pmmm, D_{2h}^1$	(1a)	Cu(t)	mmm	D_{2h}
	(1b)	O(t')	mmm	D_{2h}
	(1e)	O(t)	mmm	D_{2h}
	(1h)	Y	mmm	D_{2h}
	(2q)	Cu(m),O(b)	mm	C_{2v}
	(2r)	O(m')	mm	C_{2v}
	(2s)	O(m)	mm	C_{2v}
	(2t)	Ba	mm	C_{2v}
<i>Orthorhombic Y₂BaCuO₅ (Hazen)</i>				
$Pbnm, D_{2h}^{16}$ "Green Phase"	(4c)	Cu,Ba,Y(1),Y(2),O(3)	m	C_s
	(8d)	O(1), O(2)	1	C_1
<i>Tetragonal Bi₂Sr₂CaCu₂O₈ Tl₂Ba₂CaCu₂O₈ (Tara9, Subra)</i>				
$I4/mmm, D_{4h}^{17}$	(2a)	Ca	$4/mmm$	D_{4h}
	(4d)	O(4)	$4m2$	D_{2d}
	(4e)	Ba,Bi,Cu,O,Sr,Tl	$4mm$	C_{4v}
	(8g)	O	—	—
	(16n)	O	—	C_s

^aIn particular, sites such as Cu(t) in YBa₂Cu₃O₇ with nearest-neighbor oxygens missing have point symmetries lower than those given.

^bSee Table VI-6.

K. STRUCTURAL ORIGIN OF SUPERCONDUCTIVITY

Various types of evidence presented throughout this review support the contention that the copper oxide planes play a crucial role in the origin of the superconductivity of the LaSrCuO and YBaCuO compounds. It has also been proposed that the CuO chains are required for the superconductivity of YBaCuO (Bard1, Tora1, Vand1), perhaps through coupling to the CuO₂ planes (Engl2, Murp2). Opinions of this type were widely held prior to the discovery of the bismuth and thallium compounds described in the sections above. These new materials are tetragonal with all of the oxygen sites occupied on the CuO₂ planes, and hence no chains are present. The commonalities of these various superconductor types have been discussed (Pool5).

VII

OTHER

A. INTRODU

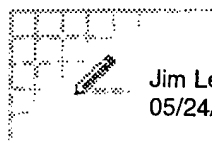
The previous c
YBaCuO, BiS
details such as
ments were str
will be treated
tropies, and la

We mention
conductors we
ties of the new
in their cation
or trivalent ca
deficiency and
begin the cha
instabilities wi
tions, the isoto
on elastic and

B. OXYGEN

The newer ox
many of the c
oxygen atoms
lated (Tara7).

ATTACHMENT B



Jim Leonard
05/24/98 02:38 PM

To: Daniel P Morris/Watson/IBM@IBMUS
cc:
From:
Subject: Layered Like or Type

Dan,

For Layered Like or Type, here are some article abstracts. One book was found for Layered Type.

Article listing are from a search of INSPEC on DIALOG.

If citation information is needed, let me know.

All the best,

Jim
James W. Leonard, Reference Librarian, Watson Library Services. Room 16-240
IBM TJ Watson Research Center,
Route 134, Yorktown Hts. NY 10598.
jwl@us.ibm.com
Voice=(914) 945 3468; Fax=(914) 945 4144

File 2:INSPEC 1969-1998/May W3
(c) 1998 Institution of Electrical Engineers

Layered like

```
?*s layered()like
      23991  LAYERED
      136878 LIKE
      S13      5  LAYERED()LIKE
?*s s13 and py=1969:1985
      5  S13
      2642109 PY=1969 : PY=1985
      S14      1  S13 AND PY=1969:1985
?*t 14/7/1
```

14/7/1
DIALOG(R)File 2:INSPEC
(c) 1998 Institution of Electrical Engineers. All rts. reserv.

02401641 INSPEC Abstract Number: A85032877
Title: Polymorphism of diphthalocyanine-neodymium. Molecular and crystal structure of beta phase
Author(s): Darovskikh, A.N.; Tsytsenko, A.K.; Frank-Kamenetskaya, O.V.; Fundamenskii, V.S.; Moskalev, P.N.

Author Affiliation: Inst. of Nucl. Phys., Acad. of Sci., Leningrad, USSR
 Journal: Kristallografiya vol.29, no.3 p.455-61
 Publication Date: May-June 1984 Country of Publication: USSR
 CODEN: KRISAJ ISSN: 0023-4761
 Translated in: Soviet Physics - Crystallography vol.29, no.3 p.273-6
 Publication Date: May-June 1984 Country of Publication: USA
 CODEN: SPHCA6 ISSN: 0038-5638
 U.S. Copyright Clearance Center Code: 0038-5638/84/030273-04\$03.90
 Language: English Document Type: Journal Paper (JP)
 Treatment: Experimental (X)

Abstract: X-ray structural analysis reveals that diphthalocyanine-neodymium, with the composition $\text{PcNdPc}/\text{sub ox/}$ ($\text{Pc} = (\text{C}/\text{sub } 32/\text{H}/\text{sub } 16/\text{N}/\text{sub } 8)/\text{sup } 2-/$, $\text{Pc}/\text{sub ox/} = (\text{C}/\text{sub } 32/\text{H}/\text{sub } 16/\text{N}/\text{sub } 8)/\text{sup } 1-/$) exists in three polymorphic modifications-tetragonal alpha, orthorhombic gamma, and monoclinic beta. Determination of the crystal structure of the beta phase ($\text{P2}/\text{sub } 1/$ automatic diffractometer, theta-2 theta method, Mo K alpha, $R=0.052$) revealed that it is of the structural type $\text{Pc}/\text{sub } 2/\text{U}$. The sandwich molecules are packed in layers parallel to the ac plane. The metal-ligand distance in the structure of $\text{Pc}/\text{sub } 2/\text{M}$ (where M is a metal ion) is explained by the ratio between the ionic radii ($r/\text{sub Nd}/>r/\text{sub u}/>r/\text{sub Sn/}$). The angle of relative rotation of the ligands is apparently determined by the character of the packing. Comparing the identity periods $\text{T}/\text{sub perpendicular to / perpendicular to the layers of molecules in the alpha, beta, and gamma modifications of diphthalocyanine-neodymium}$ ($2\text{T}/\text{sup alpha //sub (001)}/=\text{T}/\text{sup beta //sub (001)}/\sin \beta=\text{T}/\text{sup gamma //sub (101)}/$), one sees that the M-ligand distances are stable in these structures. The relation between the periods $\text{T}/\text{sup beta //sub (100)}/$ approximately= $\text{T}/\text{sup beta //sub (010)}/$ approximately= $1/2\text{T}/\text{sub (110)}/\text{sup alpha /}$ in the alpha and beta phases shows that the tetragonal structure is evidently layered like the beta phase. (10 Refs)

Layered type

```
?*s layered()type
      23991 LAYERED
      419473 TYPE
      S15      80 LAYERED()TYPE
?*s s15 and py=1969:1985
      80 S15
      2642109 PY=1969 : PY=1985
      S16      15 S15 AND PY=1969:1985
?*t 16/7/1-15
```

16/7/1
 DIALOG(R)File 2:INSPEC
 (c) 1998 Institution of Electrical Engineers. All rts. reserv.

02616964 INSPEC Abstract Number: B86015292
 Title: A study of the breakdown mechanism in dual-layer MOS capacitor dielectrics
 Author(s): Domangue, E.; Hickman, T.; Pyle, R.; Rivera, R.
 Author Affiliation: Motorola Inc., Austin, TX, USA
 Conference Title: 35th Electronic Components Conference (Cat. No. 85CH2184-0) p.396-9
 Publisher: IEEE, New York, NY, USA
 Publication Date: 1985 Country of Publication: USA 516 pp.
 U.S. Copyright Clearance Center Code: 0569-5503/85/0000-0396\$01.00
 Conference Sponsor: IEEE; Electron. Ind. Assoc
 Conference Date: 20-22 May 1985 Conference Location: Washington, DC, USA

Language: English Document Type: Conference Paper (PA)

Treatment: Experimental (X)

Abstract: The time to break down distribution of MOS capacitors fabricated with a multilayer dielectric was studied. The dielectric was composed of 10 nm of thermal silicon dioxide, 15 nm of LPCVD silicon nitride, and 1-3 nm of SiO₂/sub 2/ thermally grown on the Si/sub 3/N/sub 4/ layer. The test capacitor was constructed with paralleled storage cells in a 64K dynamic memory device. Various electric fields and temperatures were used to stress the layered type of capacitors and a control group consisting of the same vehicle but having a 39 nm silicon dioxide dielectric. Stressed units were physically analyzed to isolate the failure sites. The type and location of the dielectric breakdown faults were found to be similar in both types of dielectric structure. The layered dielectric demonstrated superior reliability, however, which is attributed to lower defectivity or the spatial variation of the applied electric field within the structure. (9 Refs)

16/7/2

DIALOG(R)File 2:INSPEC

(c) 1998 Institution of Electrical Engineers. All rts. reserv.

02506581 INSPEC Abstract Number: A85096207

Title: Reflectivity, joint density of states and band structure of group IVb transition-metal dichalcogenides

Author(s): Bayliss, S.C.; Liang, W.Y.

Author Affiliation: Cavendish Lab., Cambridge Univ., UK

Journal: Journal of Physics C (Solid State Physics) vol.18, no.17
p.3327-35

Publication Date: 20 June 1985 Country of Publication: UK

CODEN: JPSOAW ISSN: 0022-3719

U.S. Copyright Clearance Center Code: 0022-3719/85/173327+09\$02.25

Language: English Document Type: Journal Paper (JP)

Treatment: Experimental (X)

Abstract: Optical joint density of states (OJDOS) functions have been obtained from Kramers-Kronig analysis of reflectivity measurements for the layered-type materials TiS/sub 2/, TiSe/sub 2/, ZrS/sub 2/, ZrSe/sub 2/, HfS/sub 2/ and HfSe/sub 2/. The reflectivity measurements were made at near-normal incidence over the photon energy range 0.6-14 eV at 77K. Comparison of the OJDOS functions shows that there are many similarities in the band shapes which can be explained in terms of the amount of trigonal distortion present in the crystal lattice and the differences in binding energy of electron levels in the atoms. (9 Refs)

16/7/3

DIALOG(R)File 2:INSPEC

(c) 1998 Institution of Electrical Engineers. All rts. reserv.

02225943 INSPEC Abstract Number: A84041348, B84023254

Title: Hydriodic acid photodecomposition on layered-type transition metal dichalcogenides

Author(s): Bicelli, L.P.; Razzini, G.

Author Affiliation: Dept. of Appl. Phys. Chem., Milan Polytech., Milan, Italy

Journal: Surface Technology vol.20, no.4 p.393-403

Publication Date: Dec. 1983 Country of Publication: Switzerland

CODEN: SUTED8 ISSN: 0376-4583

U.S. Copyright Clearance Center Code: 0376-4583/83/\$3.00

Language: English Document Type: Journal Paper (JP)

Treatment: Experimental (X)

Abstract: The photodecomposition of hydriodic acid on platinized n-WSe/sub 2/ single crystals immersed in an aqueous 1 M HI solution was studied. During the photodecomposition process, hydrogen evolution only

occurred on the microscopic defects of the sample surface, whereas iodine was produced on the smooth areas where a diffuse orange-red colouring appeared. For polycrystalline specimens, however, hydrogen gas bubbles were formed over the entire surface, the rate of process being markedly slower than on single crystals. The results are discussed with the assumptions that the n-WSe/sub 2/ single crystals behave as Schottky-type photochemical diodes, that the cathodic reaction takes place on the stepped platinum-covered areas and that the anodic reaction occurs on the smooth unplatinized areas. (26 Refs)

16/7/4

DIALOG(R)File 2:INSPEC

(c) 1998 Institution of Electrical Engineers. All rts. reserv.

02085031 INSPEC Abstract Number: A83077984, B83041973

Title: Mechanistic studies of reversible layer-type electrodes

Author(s): Rouxel, J.; Molinie, P.; Top, L.H.

Author Affiliation: Lab. de Chimie des Solides, Nantes, France

Journal: Journal of Power Sources vol.9, no.3-4 p.345-57

Publication Date: April-May 1983 Country of Publication: Switzerland

CODEN: JPSODZ ISSN: 0378-7753

U.S. Copyright Clearance Center Code: 0378-7753/83/0000-0000/\$3.00

Conference Title: International Meeting on Lithium Batteries

Conference Date: 27-29 April 1982 Conference Location: Rome, Italy

Language: English Document Type: Conference Paper (PA); Journal Paper (JP)

Treatment: Theoretical (T)

Abstract: In layered type intercalation electrodes ions are stored reversibly during the functioning of secondary batteries. The behaviour of the system depends on geometrical and electronic factors. The geometrical factors are concerned with the localization of the ions in the host structure; they deal with average structure determinations and local ordering problems. The diffusion properties of the intercalated ions depend on the site geometry, the population of the Van Der Waals gap, the ionicity of the bonds in the host, the stoichiometry of the host, and the mechanical properties of its slabs. Electrons have to be accommodated by the host. The band structure of the host plays an important role in respect of the ability to intercalate, the phase limit, and the stability of the products. Metal-insulator transition may be induced. Other possible factors such as Jahn-Teller effects have also to be considered. (23 Refs)

16/7/5

DIALOG(R)File 2:INSPEC

(c) 1998 Institution of Electrical Engineers. All rts. reserv.

01994480 INSPEC Abstract Number: A83023215

Title: Structure of tungstic acids and amorphous and crystalline WO/sub 3/ thin films

Author(s): Ramans, G.M.; Gabrusenoks, J.V.; Veispals, A.A.

Author Affiliation: Inst. of Solid State Phys., P. Stucka Univ., Riga, USSR

Journal: Physica Status Solidi A vol.74, no.1 p.K41-4

Publication Date: 16 Nov. 1982 Country of Publication: East Germany

CODEN: PSSABA ISSN: 0031-8965

Language: English Document Type: Journal Paper (JP)

Treatment: Experimental (X)

Abstract: The authors compare the Raman spectra of a-WO/sub 3/ with spectra of crystalline WO/sub 3/.H/sub 2/O, WO/sub 3/.2H/sub 2/O and amorphous bulk WO/sub 3/.H/sub 2/O. It is concluded from the results that the structure of a-WO/sub 3/ films consists of a layered type structure of tungsten hydrates and of a framework structure of tungsten anhydride. The band at 590 cm/sup -1/ is attributed to stretching modes of the terminal

oxygen. By dehydration of amorphous WO/sub 3/.1.74 H/sub 2/O one can get amorphous bulk samples with a structure similar to the a-WO/sub 3/ thin films. (12 Refs)

16/7/6

DIALOG(R)File 2:INSPEC

(c) 1998 Institution of Electrical Engineers. All rts. reserv.

01973788 INSPEC Abstract Number: A83008001

Title: Synthesis of new layered-type and new mixed-layered-type bismuth compounds

Author(s): Kodama, H.; Watanabe, A.

Author Affiliation: Nat. Inst. for Res. in Inorganic Materials, Ibaraki, Japan

Journal: Journal of Solid State Chemistry vol.44, no.2 p.169-73

Publication Date: Sept. 1982 Country of Publication: USA

CODEN: JSSCBI ISSN: 0022-4596

U.S. Copyright Clearance Center Code: 0022-4596/82/110169-05\$02.00/0

Language: English Document Type: Journal Paper (JP)

Treatment: Experimental (X)

Abstract: Four new compounds, PbBi/sub 2/TiTaO/sub 8/F, PbBi/sub 2/TiNbO/sub 8/F, Bi/sub 5/Ti/sub 2/WO/sub 14/F, and Bi/sub 7/Ti/sub 5/O/sub 20/F, were prepared and identified by X-ray diffraction analysis. Two of them are new members of a family called layered bismuth compounds. The other two are new members of a family called mixed-layered bismuth compounds. Thermal properties of the new compounds were studied. Moreover, the possibility of the existence of other new members belonging to the family called mixed-layered bismuth compounds is discussed. (14 Refs)

16/7/7

DIALOG(R)File 2:INSPEC

(c) 1998 Institution of Electrical Engineers. All rts. reserv.

01891945 INSPEC Abstract Number: A82076639

Title: The phase relations in the Yb/sub 2/O/sub 3/-Fe/sub 2/O/sub 3/-MO systems in air at high temperatures (M: Co, Ni, Cu, and Zn)

Author(s): Kimizuka, N.; Takayama, E.

Author Affiliation: Nat. Inst. for Res. in Inorganic Materials, Ibaraki-ken, Japan

Journal: Journal of Solid State Chemistry vol.42, no.1 p.22-7

Publication Date: 15 March 1982 Country of Publication: USA

CODEN: JSSCBI ISSN: 0022-4596

Language: English Document Type: Journal Paper (JP)

Treatment: Experimental (X)

Abstract: The phase relations in the Yb/sub 2/O/sub 3/-Fe/sub 2/O/sub 3/-CoO system at 1350 and 1300 degrees C, the Yb/sub 2/O/sub 3/-Fe/sub 2/O/sub 3/-NiO system at 1300 and 1200 degrees C, the Yb/sub 2/O/sub 3/-Fe/sub 2/O/sub 3/-CuO system at 1000 degrees C and the Yb/sub 2/O/sub 3/-Fe/sub 2/O/sub 3/-ZnO system at 1300 degrees C were determined in air by means of a classical quenching method. New layered-type compounds, YbFeCoO/sub 4/ (a=3.4295(5) AA, c=25.198(3) AA), YbFeCuO/sub 4/ (a=3.4808(2) AA, c=24.100(2) AA), and YbFeZnO/sub 4/ (a=3.4251(2) AA, c=25.282(2) AA), which are isomorphous with YbFe/sub 2/O/sub 4/ (space group: R3m; a=3.455(1) AA, c=25.109(2) AA), and a new compound, Yb/sub 2/Cu/sub 2/O/sub 5/, were obtained. In the Yb/sub 2/O/sub 3/-Fe/sub 2/O/sub 3/-NiO system, there are no quaternary compounds. (10 Refs)

16/7/8

DIALOG(R)File 2:INSPEC

(c) 1998 Institution of Electrical Engineers. All rts. reserv.

01816212 INSPEC Abstract Number: C82012609

Title: Office automation technology-storage and retrieval of information

Author(s): Kurachi, T.

Author Affiliation: Toshiba Corp., Ome-shi, Japan

Journal: Journal of the Institute of Electronics and Communication Engineers of Japan vol.64, no.2 p.143-9

Publication Date: Feb. 1981 Country of Publication: Japan

CODEN: IECJAJ ISSN: 0373-6121

Language: Japanese Document Type: Journal Paper (JP)

Treatment: Applications (A); Practical (P)

Abstract: The file compositions ordered using link and direct using a page map and B tree type retrieval order are described. Layered type data models as in IBM's IMS, and the MRI System 2000, network type data models as in GE's IDS and Cineam Systems' TOTAL, relational type data model as in IBM's System R and Software AG's ADABAS and distributed type data base are also described. The types of retrieval and their call words are discussed and exemplified. Floppy disc, magnetic drum, magnetic disk, large capacity memory devices and backend systems and database machines are discussed. Micrographics and graphic information files are briefly discussed. (13 Refs)

16/7/9

DIALOG(R)File 2:INSPEC

(c) 1998 Institution of Electrical Engineers. All rts. reserv.

01587609 INSPEC Abstract Number: A80098966

Title: A method of measurement of the refractive indices of crystals with layered structure

Author(s): Allakhverdiev, K.R.; Guliev, R.I.; Salaev, E.Yu.; Kulevskii, L.A.; Savelev, A.D.; Smirnov, V.V.

Author Affiliation: Inst. of Phys., Acad. of Sci., Baku, Azerbaidzhan SSR, USSR

Journal: Physica Status Solidi A vol.60, no.1 p.309-12

Publication Date: 16 July 1980 Country of Publication: East Germany

CODEN: PSSABA ISSN: 0031-8965

Language: English Document Type: Journal Paper (JP)

Treatment: New Developments (N); Experimental (X)

Abstract: A method of determining the refractive indices of the ordinary (n_o) and extraordinary (n_e) rays in crystals with layered type structure are described. The refractive indices of layered CdInGaS₄ and TlInS₂ are measured using this technique with the help of laser radiation source at 0.63, 1.15, and 3.39 μ m. The experimentally obtained values of n_o and n_e are extrapolated from 0.6 to 4.0 μ m by the formulas $n_o/\sup 2 = A + B(\lambda/\sup 2 + C)$; $n_e/\sup 2 = K + L/(\lambda/\sup 2 + M)$. The values of the extrapolation coefficients A, B, C, K, L, and M for CdInGaS₄ and TlInS₂ crystals are obtained using the electronic computer Mir-2. (4 Refs)

16/7/10

DIALOG(R)File 2:INSPEC

(c) 1998 Institution of Electrical Engineers. All rts. reserv.

01496111 INSPEC Abstract Number: B80019231

Title: Fabrication of 8 turn multi-track thin film heads

Author(s): Hanazono, M.; Kawakami, K.; Narishige, S.; Asai, O.; Kaneko, E.; Okuda, K.; Ono, K.; Tsuchiya, H.; Hayakawa, W.

Author Affiliation: Hitachi Res. Lab., Hitachi Ltd., Ibaraki, Japan

Journal: IEEE Transactions on Magnetics vol.MAG-15, no.6 p.1616-18

Publication Date: Nov. 1979 Country of Publication: USA

CODEN: IEMGAQ ISSN: 0018-9464

Conference Title: Joint INTERMAG-MMM Conference

Conference Sponsor: IEEE

Conference Date: 17-20 July 1979 Conference Location: New York, NY, USA

Language: English Document Type: Conference Paper (PA); Journal Paper (JP)

Treatment: Practical (P)

Abstract: To obtain high bit and high track densities, fabrication of thin film magnetic recording heads have been studied by a number of companies. The authors describe a newly developed method for fabricating layered type, multi-turn, multi-track thin film inductive heads with a central tap by using photolithographic and thin film deposition techniques. (6 Refs)

16/7/11

DIALOG(R)File 2:INSPEC

(c) 1998 Institution of Electrical Engineers. All rts. reserv.

01406419 INSPEC Abstract Number: A79086309

Title: A theoretical study of the effects of various laryngeal configurations on the acoustics of phonation

Author(s): Titze, I.R.; Talkin, D.T.

Author Affiliation: Sensory Communication Res. Lab., Gallaudet Coll., Washington, DC, USA

Journal: Journal of the Acoustical Society of America vol.66, no.1

p.60-74

Publication Date: July 1979 Country of Publication: USA

CODEN: JASMAN ISSN: 0001-4966

Language: English Document Type: Journal Paper (JP)

Treatment: Theoretical (T)

Abstract: Simulation of glottal volume flow and vocal fold tissue movement was accomplished by numerical solution of a time-dependent boundary value problem in which nonuniform, orthotropic, linear, incompressible vocal fold tissue media were surrounded by irregularly shaped boundaries, which were either fixed or subject to aerodynamic stresses. Spatial nonuniformity of the tissues was of the layered type, including a mucosal layer, a ligamental layer, and muscular layers. Orthotropy was required to stabilize the vocal folds longitudinally and to accommodate large variations in muscular stress. Incompressibility and vertical motions at the glottis played an important role in producing and sustaining phonation. A nominal configuration for male fundamental speaking pitches was selected, and the regulation of fundamental frequency, intensity, average volume flow, and vocal efficiency was investigated in terms of variations around this nominal configuration. Vocal intensity and efficiency are shown to have local maxima as the configurational parameters are varied one at a time. It appears that oral acoustic power output and vocal efficiency can be maximized by proper adjustments of longitudinal tension of nonmuscular (mucosal and ligamental) tissue layers in relation to muscular layers. Quantitative verification of the 'body-cover' theory is therefore suggested, and several further implications with regard to control of the human larynx are considered. (17 Refs)

16/7/12

DIALOG(R)File 2:INSPEC

(c) 1998 Institution of Electrical Engineers. All rts. reserv.

01295844 INSPEC Abstract Number: A79010903

Title: Optical phonons in TlInS/sub 2/

Author(s): Allakhverdiev, K.R.; Adigezalov, U.V.; Nani, R.Kh.; Yusifov, Yu.G.

Journal: Izvestiya Akademii Nauk Azerbaidzhanskoi SSR, Seriya Fiziko-Tekhnicheskikh i Matematicheskikh Nauk no.1 p.21-5

Publication Date: 1978 Country of Publication: USSR

CODEN: IAFMAF ISSN: 0002-3108

Language: Russian Document Type: Journal Paper (JP)

Treatment: Experimental (X)

Abstract: The optical phonons of a wide gap semiconducting $\text{TlInS}/\text{sub } 2/$ which has a layered type structure have been investigated by the method of long-wavelength infra-red (JR) and Raman scattering spectroscopy. The splitting of absorption bands is observed when the crystals are cooled down to 100K. The comparison of phonon frequencies determined from JR and Raman experiments revealed $\text{TlInS}/\text{sub } 2/$ to be centrosymmetric. (10 Refs)

16/7/13

DIALOG(R)File 2:INSPEC

(c) 1998 Institution of Electrical Engineers. All rts. reserv.

01081136 INSPEC Abstract Number: A77063130

Title: Field dependence of the susceptibility maximum for two-dimensional antiferromagnet

Author(s): Mostafa, M.F.; Semary, M.A.; Ahmed, M.A.

Author Affiliation: Dept. of Phys., Faculty of Sci., Cairo Univ., Cairo, Egypt

Journal: Physics Letters A vol.61A, no.3 p.183-4

Publication Date: 2 May 1977 Country of Publication: Netherlands

CODEN: PYLAAG ISSN: 0375-9601

Language: English Document Type: Journal Paper (JP)

Treatment: Experimental (X)

Abstract: The magnetic susceptibility measurements on layered type structure $(\text{CH}/\text{sub } 3/\text{NH}/\text{sub } 3/)/\text{sub } 2/\text{FeCl}/\text{sub } 2/\text{Br}/\text{sub } 2/$ revealed a transition temperature $T/\text{sub } N/(H=0)$ approximately=100K. The transition temperature of $(\text{CH}/\text{sub } 3/\text{NH}/\text{sub } 3/)/\text{sub } 2/\text{FeCl}/\text{sub } 4/$ was previously found to be $T/\text{sub } N/(H=0)$ approximately=95K. The effect of magnetic field on the transition temperature and peak intensity for both compounds has been investigated. (7 Refs)

16/7/14

DIALOG(R)File 2:INSPEC

(c) 1998 Institution of Electrical Engineers. All rts. reserv.

00360679 INSPEC Abstract Number: A72019924

Title: Magnetic ordering in $\text{LiCr}/\text{sub } 1-x/\text{Fe}/\text{sub } x/\text{O}/\text{sub } 2/$

Author(s): Tauber, A.; Moller, W.M.; Banks, E.

Author Affiliation: US Army Electronics Command, Fort Monmouth, N.J., USA

Journal: Journal of Solid State Chemistry vol.4, no.1 p.138-52

Publication Date: Jan. 1972 Country of Publication: USA

CODEN: JSSCBI ISSN: 0022-4596

Language: English Document Type: Journal Paper (JP)

Treatment: Experimental (X)

Abstract: Magnetic ordering in the $\text{LiCr}/\text{sub } 1-x/\text{Fe}/\text{sub } x/\text{O}/\text{sub } 2/$ system has been investigated for polycrystal and single crystal specimens characterized by optical and X-ray diffraction techniques. Part of the $\text{Li}/\text{sub } 2/\text{O}/\text{Fe}/\text{sub } 2/\text{O}/\text{sub } 3/-\text{Cr}/\text{sub } 2/\text{O}/\text{sub } 3/$ system was also investigated. Magnetization and susceptibility measurements from 4.2 to 900K and Mossbauer measurements from 4.2 to 300K indicate that all compositions of ordered rocksalt (space group $R3m$) order antiferromagnetically at low temperatures. The first-order phase transition tracked with all Mossbauer parameters. The Weiss molecular field theory for a layered-type antiferromagnet was fitted with two exchange constants. The dependence of θ on x was found to be $\theta = \theta_a / \text{sub } a/(1-x)/\text{sup } 2/ + \theta_b / \text{sub } b/2x(1-x) + \theta_c / \text{sub } c/x/\text{sup } 2/$, where $\theta_a = \theta_a / \text{sub } a/=Cr/\text{sup } 3+/-Cr/\text{sup } 3+/-$ interaction, $\theta_b = \theta_b / \text{sub } b/=Fe/\text{sup } 3+/-Cr/\text{sup } 3+/-$ interaction and $\theta_c = \theta_c / \text{sub } c/=Fe/\text{sup } 3+/-Fe/\text{sup } 3+/-$ interaction. A spontaneous magnetization associated with iron-substituted crystals originated with an epitaxial overgrowth of $\text{LiCr}/\text{sub } 4.75/\text{Fe}/\text{sub } 0.25/\text{O}/\text{sub } 2/$

8/. (29 Refs)

16/7/15
DIALOG(R)File 2:INSPEC
(c) 1998 Institution of Electrical Engineers. All rts. reserv.

00301052 INSPEC Abstract Number: C71019443
Title: A static and dynamic finite element shell-analysis with
experimental verification
Author(s): Klein, S.
Author Affiliation: Aerospace Corp., San Bernardino, CA, USA
Journal: International Journal for Numerical Methods in Engineering
vol.3, no.3 p.299-316
Publication Date: July-Sept. 1971 Country of Publication: UK
CODEN: IJNMBH ISSN: 0029-5981
Language: English Document Type: Journal Paper (JP)
Treatment: Theoretical (T)

Abstract: A system of finite element shell analysis codes, called
SABOR/DRASTIC, is used to analyse a complex two-layered shell of revolution
under static and dynamic asymmetric loads. The dynamic analysis is compared
with experimentally measured response. In this linear elastic analysis,
emphasis is placed on the inherent flexibility of the finite element method
in modelling the complex structural geometry of a given test specimen.
Static studies, which involve variations in important shell parameters, and
dynamic studies, which provide a successful correlation with experiment,
are used to illustrate both the detail and the generality with which shell
analyses may now be performed with confidence.

Layered Like books = 0

43=> f (layered-like) or (layered w like)

Searching ...

S E A R C H R E S U L T S

Search ID	Records Found	Search Term
S43	0	layered-like
S44	1440	layered
S45	57219	like
S46	0	(layered-like) or (layered w like)

Layered Type books = 1

47=> f (layered-type) or (layered w type)

Searching ...

S E A R C H R E S U L T S

Search ID	Records Found	Search Term
-----------	---------------	-------------

S47 0 layered-type
S48 1440 layered
S49 82277 type
S50 1 (layered-type) or (layered w type)

51=> f s50 and yr < 1986

Searching ...

S E A R C H R E S U L T S

Search ID	Records Found	Search Term
-----	-----	-----

S51	1	s50 and yr < 1986
-----	---	-------------------

52=> d s51 1 f8

R e c o r d 1 o f 1

Copyright 1998 OCLC

Page: 1 of 1

AN: 23935341

AU: Lee, Harry Nai-Shee, 1942-

TI: Electrical transport properties of some hexagonal layered type transition metal chalcogenides.

YR: 1969

LN: English

PT: Book

PH: ix, 83 l. charts, diagrs. 28 cm.

**This Page is Inserted by IFW Indexing and Scanning
Operations and is not part of the Official Record**

BEST AVAILABLE IMAGES

Defective images within this document are accurate representations of the original documents submitted by the applicant.

Defects in the images include but are not limited to the items checked:

- ☐ **BLACK BORDERS**
- ☐ **IMAGE CUT OFF AT TOP, BOTTOM OR SIDES**
- ☐ **FADED TEXT OR DRAWING**
- ☐ **BLURRED OR ILLEGIBLE TEXT OR DRAWING**
- ☐ **SKEWED/SLANTED IMAGES**
- ☐ **COLOR OR BLACK AND WHITE PHOTOGRAPHS**
- ☐ **GRAY SCALE DOCUMENTS**
- ☐ **LINES OR MARKS ON ORIGINAL DOCUMENT**
- ☐ **REFERENCE(S) OR EXHIBIT(S) SUBMITTED ARE POOR QUALITY**
- ☐ **OTHER:** _____

IMAGES ARE BEST AVAILABLE COPY.

As rescanning these documents will not correct the image problems checked, please do not report these problems to the IFW Image Problem Mailbox.